c-axis optical spectra and charge dynamics in $La_{2-x}Sr_xCuO_4$

S. Uchida and K. Tamasaku
Department of Superconductivity, University of Tokyo, Yayoi 2-11-16, Bunkyo-ku, Tokyo 113, Japan

S. Tajima
Superconductivity Research Laboratory, ISTEC, Shinonome 1-10-13, Koto-ku, Tokyo 135, Japan
(Received 16 November 1995; revised manuscript received 7 February 1996)

Out-of-plane (c-axis-polarized) optical reflectivity spectra and c-axis charge transport properties are studied for single crystals of a high-T_c system $La_{2-x}Sr_xCuO_4$ over a wide compositional range $0 \leqslant x \leqslant 0.30$. The measurements are made at various temperatures in the normal and superconducting states over an energy range from 0.003 to 40 eV. The present study focuses on the evolution of the c-axis spectrum with doping and provides a full set of the optical and transport data on this single-layer system together with the previously published data of the in-plane spectra [S. Uchida *et al.*, Phys. Rev. B **43**, 7942 (1991)]. As in the case of the in-plane spectrum, the spectral weight is transferred upon doping from the high- to low-energy region. Different from the in-plane spectrum the transferred weight forms a band which is centered at relatively high energy ($\sim$ 2 eV) and does not appreciably move with increasing x. As a consequence, the c-axis optical conductivity [$\sigma_c(\omega)$] is extremely small in the lowest-energy region (<0.3 eV) until the compound is overdoped. Particularly, in the underdoped regime ($x<0.13$) the low-energy $\sigma_c(\omega)$ is too small to form a Drude peak, and is further suppressed with reducing temperature. This is in common with the pseudogap effect, observed for the bilayer system $YBa_2Cu_3O_{6+x}$, and is connected to the semiconducting c-axis resistivity. A Drude peak in $\sigma_c(\omega)$ develops only in the highly doped compounds ($x \geqslant 0.18$). Only in the overdoped regime is $\sigma_c(\omega)$ dominated by a sharp Drude term and the anisotropic resistivity ρ_c/ρ_{ab} almost constant over a wide temperature range, giving strong evidence for a three-dimensional metallic state. In the superconducting state the c-axis infrared optical response is quite anomalous as it is characterized by a sharp plasma edge. In the underdoped regime, the strongly suppressed spectral weight in the normal state gives rise to a sharp plasma edge within a gap region, which can be identified as a Josephson plasma in the weakly Josephson-coupled layered superconductor. In the highly doped superconducting regime, an appreciable Drude-like component remains in the spectrum even at temperatures well below T_c, leading to a substantial damping of the Josephson plasma. Such a gapless spectrum is perhaps associated with a crossover from the underdoped to the nonsuperconducting overdoped regime. [S0163-1829(96)01821-8]

I. INTRODUCTION

The infrared (IR) optical spectrum has successfully been used to study exotic ground states of recently discovered novel metals such as charge or spin density waves,[1] dense Kondo state of heavy fermions,[2] and oxide superconductors with low density of states.[3] Soon after the discovery of high-temperature superconductivity (HTSC) in copper oxide systems,[4] a number of optical experiments have been done to unravel the electronic state which gives birth to the unprecedently high-T_c superconductivity.[5] However, the optical spectra, in particular the infrared spectra, are much more complicated beyond the researchers expectations. The complications arise mainly from (i) strong anisotropy in the properties parallel and perpendicular to the CuO_2 planes which are the key structural element of HTSC, and (ii) extreme sensitivity of the properties to the compositions (stoichiometry) which control the carrier density in the CuO_2 plane. These difficulties lead to much confusion in the understanding of the electronic state as well as superconducting gaps of HTSC.

Considerable progress was made in single-crystal growth at around 1989. Since then, most of the previous data on ceramic samples have been replaced by the data on single crystals, and many of the controversies have been resolved concerning the in-plane optical spectra.[6] The quality of the crystals has progressively been improved, and now single crystals with well-controlled compositions (stoichiometry) have become available for experimentalists.[7] This has allowed them to investigate the evolution of the optical properties with doping which has accelerated the understanding of the electronic state of the doped carriers in the CuO_2 plane.[8–12]

Furthermore, since 1992, thick single crystals have been successfully grown at several research groups, and the out-of-plane optical properties are now being intensively investigated to understand the interplane charge dynamics of HTSC. As shown in Fig. 1, the magnitude of the out-of-plane resistivity (ρ_c) differs by more than three orders among various cuprate materials near optimal doping.[13] This is in sharp contrast to the in-plane resistivity (ρ_{ab}) which has nearly the same magnitude in the normal-state values and T-linear coefficient near optimal doping.[14] The band theoretical calculations can explain, to some extent, the difference in ρ_c as the difference in the band dispersion along the c direction.[15] However, the band calculations always predict an appreciable c-axis dispersion and thus an anisotropic three-dimensional metallic state. It has often been pointed out that

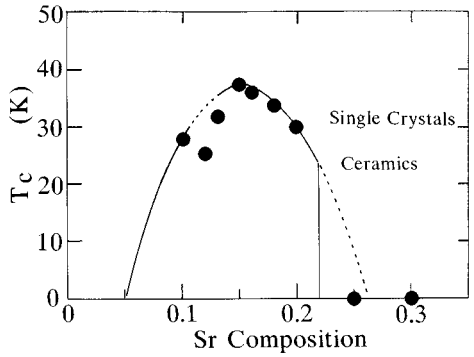

FIG. 1. Critical temperature (T_c) plotted as a function of x for the $La_{2-x}Sr_xCuO_4$ single crystals used in the present study. The solid (dotted in parts) curve is the x dependence of T_c for well-characterized ceramics (Refs. 23 and 28). The vertical line at $x = 0.22$ indicates the tetragonal-orthorhombic phase boundary which also separates the superconducting and overdoped metallic phase. A dip at $x = 0.12$ is a consequence of the T_c suppression near $x = 1/8$ in La-based cuprates.

evidence in support of the band picture is the metallic T dependence of ρ_c observed for the fully oxygenated $YBa_2Cu_3O_7$,[16] which forms the most stoichiometric and perfect crystal among the known high-T_c cuprates.

By contrast, there are theories which presume two-dimensional electronic state realized due to electronic correlations. An example is the resonating-valence-bond (RVB) theory[17] which predicts that the charge carriers are confined within the CuO_2 plane, allowing for no coherent motion between the planes. Actually, there is a general trend that the cuprates in the underdoped regime show nonmetallic ρ_c with negative T coefficient ($d\rho_c/dT < 0$).[18,19] Therefore, in order to understand the charge dynamics in the c direction it is necessary to study the out-of-plane optical spectrum of HTSC as a function of dopant concentration. At present this is possible only on $La_{2-x}Sr_xCuO_4$ (La214) system for which large high-quality single crystals are available over a wide compositional range. We show below how the out-of-plane optical spectrum evolves with doping for La214 which will clarify the dimensionality of the electronics as well as the out-of-plane charge dynamics. We expect that the results would be universal for all the high-T_c cuprates irrespective of the number of CuO_2 planes in a unit cell.

In the superconducting state an enormous number of infrared studies have thus far been carried out on the high-T_c cuprates as a standard technique that is much less sensitive to sample surface compared to other techniques.[20] Nevertheless, the magnitude and symmetry of the superconducting gap are still controversial. This is partly because the in-plane infrared reflectivity is close to unity and thus high accuracy is required to defect a very small change occurring across T_c. Because of the strong anisotropy this is not the case with the out-of-plane spectrum. Tamasaku *et al.*[21] have clearly demonstrated a remarkable charge in the out-of-plane reflectivity spectrum at T_c. A sharp reflectivity edge appearing below T_c in the very-low-frequency region was assigned to the plasma edge of the carriers condensed into the superconducting state. The plasma frequency, determined by the weight of a δ function at $\omega=0$ in the optical conductivity spectrum, directly gives the out-of-plane London magnetic penetration depth. It was also noted that such an anomalous optical response can happen when the superconducting gap is larger than the plasma frequency. Since the La214 system has only one CuO_2 plane per unit cell and the coupling between the planes would be weak, there would be only one energy scale in the superconducting state, a gap associated with in-plane pairing, which will be relevant to the optical response for any polarization. Therefore, we expect that the study of the doping dependence of the out-of-plane optical response will yield information on how the superconducting gap of HTSC evolves with doping as well as how the out-of-plane London length varies with doping.

In this paper the experimental results of HTSC are presented for $La_{2-x}Sr_xCuO_4$, a prototype HTSC, emphasizing the evolution of the out-of-plane optical spectrum with doping. In Sec. II we describe the crystal growth and characterization of single crystals used for the measurements of the out-of-plane properties. Section III reviews the in-plane spectrum in the normal state which shows a remarkable and characteristic change with doping. The out-of-plane optical spectrum in the normal state is presented in Sec. IV. Central concerns are the two dimensionality of the electronic state and the charge transport mechanism between the CuO_2 planes.

Section V deals with the out-of-plane optical spectra in the superconducting state, and addresses the gap structure and the phenomenon so-called Josephson plasma. The focus is again on the evolution of the gap and the plasma frequency with doping. We conclude in Sec. VI with emphasis on the unique and characteristic electronic state of HTSC which can be deduced from the out-of-plane optical spectra.

II. SAMPLE CHARACTERIZATION

La214 single crystals with various Sr compositions ($x =$ 0, 0.10, 0.12, 0.13, 0.15, 0.16, 0.18, 0.20, 0.25, and 0.30) were grown by the traveling-solvent-floating-zone (TSFZ) method.[22] The details of crystal growth and characterization by resistivity and magnetization measurements were described in Ref. 19. Evidence for the high quality of the present crystals is seen in the T_c-x diagram shown in Fig. 1 which indicates that the x dependence of T_c coincides exactly with that established for the best-characterized ceramic samples.[23,24] The points that should be marked in this diagram are the following.

(i) The temperature dependence of the c-axis resistivity (ρ_c) shows a kink for $x \leqslant 0.20$ at the temperature T_0 corresponding to the tetragonal-orthorhombic structural phase transition. The values of T_0 and the x dependence of T_0, which were also determined using high-resolution dilatometry method, are exactly the same as those reported previously.[25]

(ii) The detailed phase diagram of La214 has characteristic singularities at $x \sim 0.12$ and 0.22. The former is related with the so-called ''1/8'' anomaly — associated with the second tetragonal phase transition in the case of $La_{2-x}Ba_xCuO_4$ — at which superconducting is severely suppressed.[26] The ground state at this composition is perhaps an antiferromagnetic (AF) insulator. If there should be an inevitable inhomogeneous distribution of Sr content in this

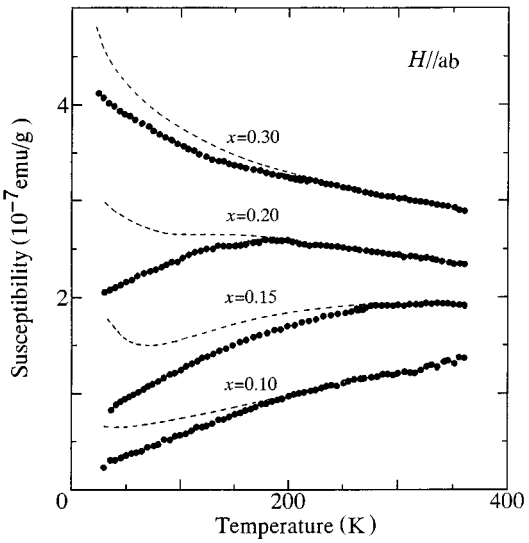

FIG. 2. Temperature dependence of the normal-state magnetic susceptibility of La214 single crystals with magnetic field applied parallel to the *a*-*b* plane. The dashed curves are the results for as-grown crystals.

solid solution system, the compound near $x\sim 0.12$ would be magnetically contaminated due to this AF phase. Actually, neutron scattering and muon-spin-relaxation (μSR) experiments on earlier La214 single crystals with $x\sim 0.15$ showed an indication of magnetic contamination[27] and there appeared a Curie component in the static magnetic susceptibility. The Curie term in the present crystal with $x=0.15$ is strongly reduced (Fig. 2) and the preliminary neutron and μSR measurements on the same crystals show very tiny trace of the contamination.[27]

(iii) The singularity at $x\sim 0.22$ corresponds to the phase boundary $T_0 = 0$, which incidentally coincides with the boundary between superconducting and nonsuperconducting metallic phases.[28] Inhomogeneous crystals would show appreciable superconducting volume fraction even at the composition well higher than $x = 0.22$. As we shall see in Sec. V D, the present crystal with $x = 0.25$ shows no bulk superconductivity. These results guarantee that the Sr composition is well controlled in our crystals and Sr atoms (as well as oxygen content) are homogeneously distributed over a crystal.

III. REVIEW OF IN-PLANE OPTICAL SPECTRUM

A. In-plane optical conductivity spectrum near optimal doping

Before we go into details of the out-of-plane optical spectrum, we review the characteristic features of the in-plane spectrum which have been almost established. This would be helpful to highlight a remarkable difference in the spectral features and charge dynamics between the two directions. The in-plane optical conductivity spectra of various cuprate materials near optimal doping ($x\sim 0.2$) have common features,[20] a sharp peak at $\omega = 0$ and a long tail extending to higher frequencies in the infrared (IR) region where $\sigma(\omega)$ falls as ω^{-1} slower than ω^{-2} decay in the Drude spectrum: (i) ''one-component'' analysis in which both the sharp peak and long tail are due to the same carriers with strongly ω-dependent scattering rate and effective mass; (ii) the ''two-component'' picture in which the $\sigma(\omega)$ spectrum is decomposed into a Drude peak at $\omega=0$ and an absorption band centered at ω in the mid-IR region, the so-called mid-IR absorption band.[6,29]

In the one-component picture, the scattering rate $1/\tau$ has to increase rapidly with ω, so that a small $1/\tau$ is responsible for the sharp peak at $\omega=0$ in $\sigma(\omega)$ and a large $1/\tau$ for the long tail at higher frequency. As an empirical approach one can determine the ω-dependent scattering rate $\tau^{-1}(\omega)$ [as well as $m^*(\omega)$] from the experimental optical data based on the generalized Drude formalism[30]

$$\sigma(\omega)=\frac{\omega_p^2}{4\pi}\frac{m}{m^*(\omega)}\frac{\tau(\omega)}{[1-i\omega\tau(\omega)]}, \tag{1}$$

where an ω-dependent effective mass is introduced to satisfy causality [i.e., Kramers-Kronig relations between $\tau^{-1}(\omega)$ and $m/m^*(\omega)$]. Many groups have determined $\tau^{-1}(\omega)$ using this approach and found that τ^{-1} appears to depend linearly on ω for various cuprates with near optimal composition, just in accordance with the T-linear resistivity ($\rho\sim\tau^{-1}\sim T$).[30] This result might lead to the conclusion that the scattering rate $1/\tau$ is linear in T at low ω and linear in ω at T which gives a basis for various theoretical models of HTSC.[31-34]

In the two-component picture, a Drude component gives a sharp peak at $\omega = 0$ and a mid-IR component is responsible for a long tail at high frequencies. One might suppose that the Drude and mid-IR terms represent the contribution from the free carriers and the bound electrons, respectively. The Drude carriers couple only weakly with phonons or other excitations (coupling constant $\lambda\lesssim 0.3$) which gives rise to a sharp $\sigma(\omega)$ peak at $\omega = 0$ as well as the T-linear resistivity persisting to 1000 K or higher.[35] The T-linear resistivity is assumed to arise from the linear-T dependence of $1/\tau$ which is independent of ω, and the magnitude of resistivity is given by $\rho=4\pi/\omega_{pD}^2\tau$, where ω_{pD} is the plasma frequency of the Drude free carriers and substantially smaller than ω_p in the ''one-component'' analysis.

B. Evolution of the in-plane spectrum with doping

The $\sigma(\omega)$ spectra demonstrate what is going on as doping proceeds. The undoped compound is characterized by charge transfer (CT) excitations peaked at $\sim$ 2 eV which correspond to the optical transitions across a CT gap formed between occupied O $2p$ band and empty Cu $3d$ upper Hubbard band. Upon doping, the low-energy conductivity increases below $\sim$ 1.2 eV, whereas the intensity of the CT band is reduced. The analysis of the sum-rule [or $N_{\rm eff}(\omega)$], the total spectral weight below 3–4 eV being nearly unchanged before and after doping, leads to a conclusion that the spectral weight of the CT excitation is transferred to the low-energy excitations. Essentially the same phenomenon has been observed for other cuprate materials.[8-12]

A physical implication of these results is that doped holes (electrons) are not free particles in the O $2p$ valence band, but they behave like correlated particles with restrictions on double occupancy, as if holes were doped into the lower Hubbard band.[36–39] The spectral weight transfer is a general

feature of doped Mott insulators, suggesting that the doping redistributes the states which form upper and lower Hubbard bands in a parent insulator. Actually, the spectral weight transfer upon doping is also observed in other $3d$ transition-metal oxide systems.[40] What is distinct in HTSC is the very rapid transfer rate at initial dopings. This originates from a rapid development of a Drude band owing to the distinctively high itinerancy of the doped carriers in the CuO_2 plane.

At light doping levels the mid-IR band dominates in the low-energy region and a narrow Drude peak grows independently at $\omega = 0$. Thus, the two-component picture is more appropriate in this doping regime. As doping proceeds, the intensity of both components increases, but the mid-IR band shifts to lower energies, merging into one absorption band in the heavily doped region. In this regime, the one-component analysis with ω-dependent τ seems also to be a good description. It is a delicate question to ask which analysis, one component or two component, is more appropriate near the optimal doping $x \sim 0.15$.

C. In-plane charge dynamics

The weight of the Drude component in $\sigma_{ab}(\omega)$ is a measure for the itinerancy of the doped holes. For lightly doped materials the mid-IR band is obviously separated from the Drude band and overweighs the Drude one, indicating that only a part of the states is itinerant and contributes to the dc transport. On the other hand, they appear to extend over the whole band of states in the overdoped region, where the generalized Drude descriptions may be valid. The evolution of the itinerant states should be reflected in the doping dependence of the in-plane dc conductivity and reciprocal Hall coefficient. Both show strong x dependences, increasing steeply with doping in the optimally doped region.

The T-linear resistivity over a wide temperature range is observed in a narrow compositional range around the optimum doping.[19,41] It is superlinear (or quadratic in T) in the overdoped regime. In the underdoped region the in-plane resistivity shows a deviation from T-linear dependence — the resistivity appears to be reduced in the low-temperature region. The deviation from T linearity is more clearly seen in the case of $YBa_2Cu_3O_{6+x}$ (Y123).[42] For this system, particularly for the $T_c = 60$ K compound ($x \sim 0.65$), there is a strong indication in NMR (Refs. 43,44) and neutron scattering[45,46] experiments that a gap opens at $\boldsymbol{q}=\boldsymbol{Q}$, the antiferromagnetic wave vector, in the spin excitation spectrum at a temperature ($T_s \sim$ 180 K) well above superconducting T_c. Furthermore, it is suggested that the decreasing (static) magnetic susceptibility with lowering T, characteristic of the underdoped regime of all the HTSC's,[23,24,47–49] might be connected to a spin gap that opens near $\boldsymbol{q} = 0$. The decrease of the magnetic susceptibility seems to start at a temperature (T^*) higher than T_s at which a spin gap opens at $\boldsymbol{q}=\boldsymbol{Q}$. It is found that the deviation from T linearity in the resistivity starts at $T \sim T^*$ and becomes substantial at $T \sim T_s$. This correlation gives evidence for an intimate relationship between in-plane charge transport and spin fluctuations. The opening of a spin gap would lead to suppression of the carrier scattering and thus to a reduction in resistivity. In this regard, the T-linear resistivity, at optimal doping and at high temperatures for underdopings, likely arises from a coupling with a zero-gap spectrum of spin fluctuations.

The characteristic temperature T^* was also identified in magnetic susceptibitily of La214 at which χ_m shows a peak. As suggested by recent transport measurements,[50,51] T^* is a characteristic temperature separating different high- and low-temperature charge dynamics. Different from Y123, the spin gap at $\boldsymbol{q}=\boldsymbol{Q}$ or the spin gap temperature T_s has not been identified for La214, which might be a reason for the less dramatic non-T-linear resistivity in La214.

IV. OUT-OF-PLANE OPTICAL SPECTRUM IN THE NORMAL STATE

An understanding of the optical properties in such an anisotropic medium as HTSC's is not complete without an understanding of the out-of-plane optical response. In contrast to the tremendous number of experimental studies made on the in-plane properties of HTSC's, much less has been known about the properties in the direction perpendicular to the CuO_2 planes (c-axis direction). One expects anisotropic properties from the layered crystal structure, but it is not a trivial issue whether the actual electronic state is two dimensional or not and whether the frequently observed semiconducting charge transport in the c direction is intrinsic or not.

Previously it was shown for $La_{2-x}Sr_xCuO_4$,[19,52] $YBa_2Cu_3O_{6+x}$,[53] and $Bi_2Sr_2CaCu_2O_{8+x}$ (Ref. 54) that the out-of-plane resistivity ρ_c rapidly decreases with dopant concentration and the T coefficient of ρ_c changes sign from negative in the underdoped regime to positive in the overdoped regime. This trend is certainly general of all the high-T_c cuprate systems and signals a marked change in charge transport with doping. In this section we show the evolution of the out-of-plane optical spectrum with doping to clarify the dimensionality of the electronic state and the charge dynamics between the planes.

The TSFZ crystals were cut to have a surface containing c axis, and the surface was mirror polished for optical measurements. The c-axis-polarized reflectivity spectra were measured in the energy range between 0.003 and 40 eV. The infrared region was covered by a rapid-scan Fourier-type interferometer and the ultraviolet region by synchrotron radiation in the facility of the Institute for Solid State Physics, University of Tokyo.

A. Out-of-plane optical conductivity spectrum

The c-axis-polarized reflectivity spectra are shown in Fig. 3 in the wide energy range between 0.005 and 40 eV. In the high-energy region two prominent edges at $\sim$ 13 and $\sim$ 30 eV are seen, associated with the interband excitations involving La $5d/4f$–derived conduction bands and the plasma of all the valence electrons, respectively.[55]

These high-energy edges are observed in the in-plane spectrum at nearly the same energies, and so the spectrum above 5 eV is nearly isotropic. On the other hand, the low-energy spectrum dominated by the excitations within (or between) CuO_2 plane(s) is strongly anisotropic. While an edge at $\sim$ 1 eV appears upon doping in the in-plane spectrum, the out-of-plane spectrum is dominated by the two (three) optical phonon bands at all the compositions. The doping-

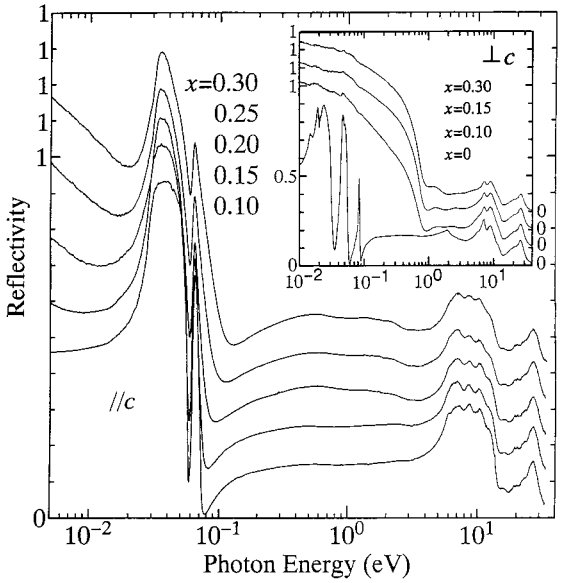

FIG. 3. c-axis reflectivity spectrum of $La_{2-x}Sr_xCuO_4$ (at room temperature) for various compositions between $x = 0.10$ and 0.30 (from bottom to top) measured over a wide energy range from far infrared to vacuum ultraviolet. The inset shows the corresponding in-plane reflectivity spectra for x between 0 and 0.30.

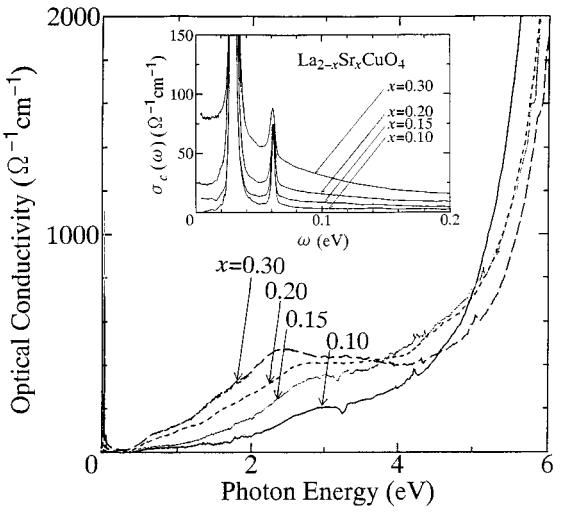

FIG. 4. Evolution of the c-axis optical conductivity spectrum below 6 eV with doping. $\sigma_c(\omega)$ is calculated via Kramers-Kronig transformation of the data shown in Fig. 3. Expanded spectra in the lowest-energy region (below 0.2 eV) are shown in the inset.

induced change in the out-of-plane spectrum is very weak. One can recognize a very weak edge at $\sim$ 2 eV and a negative slope [of $R_c(\omega)$] in the lowest-energy region developing gradually with x.

The electronic contribution to $\sigma_c(\omega)$ of the undoped ($x = 0$) compound is suppressed to almost zero up to $\sim$ 3 eV above which the high-energy interband transitions start. Unlike the in-plane spectrum of La_2CuO_4 a feature corresponding to the charge-transfer excitations involving O $2p$ and Cu $3d$ states is not clearly seen. This is consistent with the result of the c-axis-polarized x-ray-absorption spectroscopy (XAS),[56,57] indicating that the fundamental CT excitations are between the states of predominantly in-plane character (O $2p_{x,y}$ and Cu $3d_{x^2-y^2}$).

Upon doping some spectral weight in the 5–6 eV region is transferred into the low-energy region as in the case of the in-plane spectrum (Fig. 4). Similar to $\sigma_{ab}(\omega)$ in the underdoped regime, $\sigma_c(\omega)$ appears to be composed of two (or more) bands separated at $\sim$ 0.25 eV. The higher-energy band, corresponding to the ''mid-IR'' in $\sigma_{ab}(\omega)$, shows a broad peak at $\sim$ 2 eV. The weight of this band increases with x, but the peak position does not appreciably shift to lower energies, as if the ''mid-IR'' is pinned at $\sim$ 2 eV in $\sigma_c(\omega)$. On the other hand, the weight of the lower-energy band, corresponding to the Drude in $\sigma_{ab}(\omega)$, is much smaller and does not form a well-defined peak at $\omega = 0$ until the material is overdoped.[58] The very small transfer of the spectral weight below 0.25 eV is the reason for the dominance of the optical phonons in the c-axis spectrum. Since the suppression of σ_c extends over such a wide energy, it should be a purely electronic interaction effect, not a localization effect due to disorder or phonons. Plausibly, the poorly screened Coulomb interactions in the c direction would play some role. In the underdoped region ($x<0.15$) we shall see in the next section that $\sigma_c(\omega)$ in the lowest-energy region (below $\sim$ 0.1 eV) is further depressed as the temperature is lowered.

The low-energy electronic contributions to $\sigma_c(\omega)$ progressively increase and become a decreasing function of ω for higher dopant concentrations. However, the values of the optical conductivity are by orders of magnitude smaller than those of the in-plane conductivity in the corresponding energy range, and for the underdoped compounds even smaller than the critical value $\sigma_c^{\min}\sim 50\ \Omega^{-1}\mathrm{cm}^{-1}$, which corresponds to the mean free path comparable with the c-axis lattice constant.[59] $\sigma_c(\omega)$ for $x \leqslant 0.15$ is almost ω independent, so that it cannot be described by a Drude formula even if an ω-dependence of scattering rates is taken into consideration. The small value of σ_c and the absence of a Drude peak in $\sigma_c(\omega)$ are evidence of incoherent charge transport in the c direction and are consistent with nonmetallic transport in the c direction.

B. c-axis optical phonons

As seen in Figs. 5 and 6, the electronic contribution to the c-axis conductivity spectrum is so small and featureless that we can easily distinguish the phonon peaks from the observed spectrum. At room temperature in the tetragonal phase, two phonon peaks are clearly observed at 29 and 61 meV for $\mathbf{E}//c$ [according to a group theory for a crystal with D_{4h}^{17} symmetry, $\Gamma_{\mathrm{opt}}=3A_{2u}+4E_u+B_{2u}+2A_{1g}+2E_g$, there are three infrared active modes (A_{2u})]. The third phonon is clearly seen at 43 meV for $x=0.10$ as a dip superposed on the strong 29 meV band. The highest-frequency phonon mode is associated with apical oxygen vibration along the c axis, while the 29 meV peak with gigantic oscillator strength is assigned either to the La(Sr)-vibrational mode, or the in-plane oxygen bending mode (or these two might accidentally be degenerate). The peak height of this phonon reaches 1000 $\Omega^{-1}\,\mathrm{cm}^{-1}$ for $x = 0$ and 0.10. There is no evidence for a strong coupling between this mode(s) and the

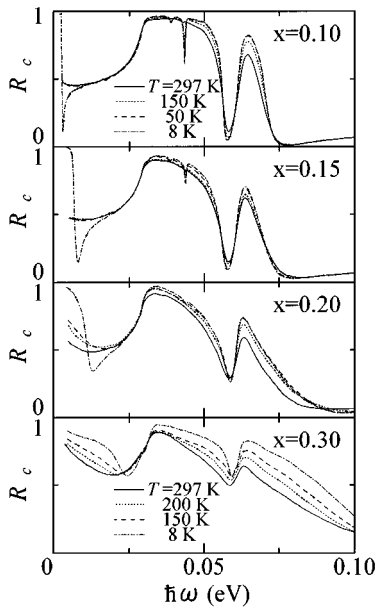

FIG. 5. Infrared c-axis reflectivity spectra below 0.1 eV at several temperatures for four compositions $x = 0.10$, 0.15, 0.20, and 0.30.

electronic background (low-energy electronic excitations) — the absorption spectrum does not show an appreciable asymmetry or a significant dependence on temperature and Sr composition. Such a strong c-axis phonon is not specific to La214 but is observed for the isostructural La_2NiO_4 and La_2CoO_4. Probably, the oscillator strength would come from higher-energy electronic excitations, reflecting strong ionic character (or poor Coulombic screening) of the La-based K_2NiF_4 structure in the c direction.

As the temperature decreases, the crystal symmetry changes from tetragonal (D_{4h}^{17}) to orthorhombic (D_{2h}^{18}) at a

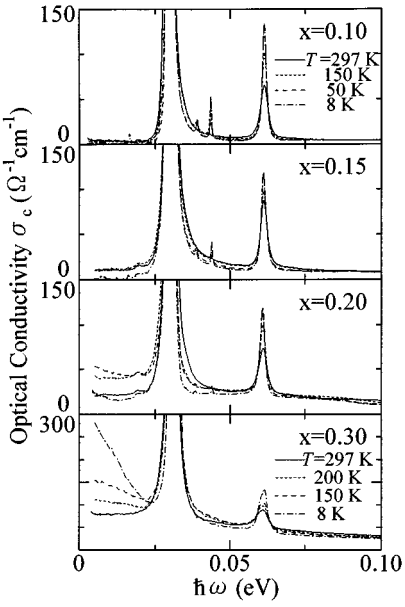

FIG. 6. c-axis optical conductivity spectra below 0.1 eV at several temperatures for four compositions $x = 0.10$, 0.15, 0.20, and 0.30.

temperature T_0, which can be also observed as a kink in the $\rho_c(T)$ curve.[19] In the orthorhombic phase, two additional phonons appear at 16 and 39 meV as most clearly seen for $x = 0.10$, reflecting a lower crystal symmetry (the phonon spectrum for $x = 0$ is essentially the same as that for $x = 0.10$).

As the Sr composition increases from $x=0.10$ to $x=0.20$, the TO-phonon frequency for the apical oxygen mode decreases by 0.4 meV, while the frequency for the in-plane oxygen mode increases by 0.3 meV. The former change may be caused by an elongation of the c axis with increasing x, although it is not consistent with the experimental observation that the bond distance between the apical oxygen and Cu decreases with increasing x.[60] The latter change, the hardening of the in-plane oxygen mode, can be understood as a result of the a-axis shortening with increasing x.

Recently several anomalies in the temperature dependence of c-axis optical phonons have been reported. One is an abrupt change in the phonon frequency and/or damping at T_c for the optimally doped $YBa_2Cu_3O_{6+x}$, which is interpreted as a superconducting gap effect on the phonon self-energy. It is observed in the Raman-active phonons but is not relevant to the infrared-active phonons.[61] Another is a remarkable softening of the in-plane oxygen mode from well above T_c observed for the underdoped bilayer systems $YBa_2Cu_3O_{6+x}$ and $YBa_2Cu_4O_8$.[65] Based on the correlation between temperature dependence of the phonon frequency and of the spin relaxation time T_1^{-1} in NMR, Litvinchuk *et al.*, claimed that this phonon softening is related to the spin gap opening via a spin-phonon coupling.[62] However, since the charge dynamics also changes dramatically with reducing temperature in the underdoped regime, it is not clear whether it is an indication of a direct coupling between phonons and spins. The third anomaly is a broad peak around 50 meV which grows at low temperatures in underdoped $YBa_2Cu_3O_{6+x}$,[63] $YBa_2Cu_4O_8$,[64] and $Pb_2Sr_2(Y,Ca)Cu_3O_8$.[65] The appearance of this new peak is a consequence of the redistribution of the phonon oscillator strength below a certain temperature. Based on the doping dependence of the onset temperature as well as the peak frequency for this anomaly, Schützmann *et al.* proposed that this anomaly is related to a spin gap.[66]

It is of great interest to check these phonon anomalies in single-layer $La_{2-x}Sr_xCuO_4$. As the temperature decreases, except for a weak softening ($\sim$ 0.2 meV) of the apical oxygen mode observed for $x=0.15$ and 0.20, all other modes show weak hardening (less than 0.6 meV) for $x = 0.10$ and 0.15, and almost no change for $x = 0.20$. The oscillator strength can be estimated accurately only for the apical oxygen mode around 61 meV, because it is isolated from the gigantic mode at 29 meV. For $x = 0.15$, the oscillator strength of the apical oxygen mode increases by 20% as the temperature is decreased from 300 to 10 K, whereas no remarkable change is observed for $x = 0.10$ and 0.20. In contrast to the phonon anomalies observed in the bilayer systems, no significant change is identified below T_c and below $T_0(\sim T^*)$. Neither spectral weight redistribution among phonons is clearly identified in $La_{2-x}Sr_xCuO_4$. This indicates that such anomalies are pronounced in the bilayer cuprates in conformity with the experimental fact that a pos-

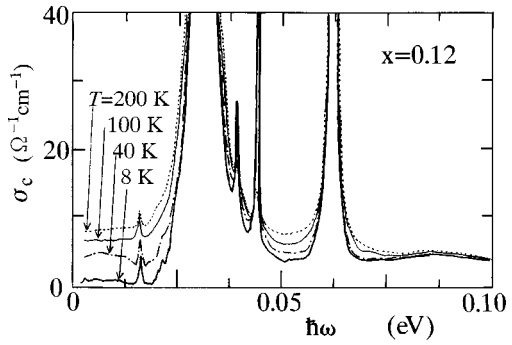

FIG. 7. $\sigma_c(\omega)$ at various temperatures for a low-doping compound, $x = 0.12$. A weak pseudogap behavior is seen in the normal state in the energy region below $\sim$ 0.1 eV.

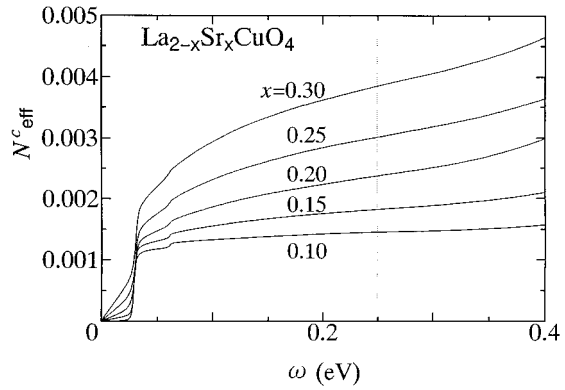

FIG. 8. Effective electron number per Cu atom ($N^c_{\rm eff}$) defined as a conductivity [$\sigma_c(\omega)$] sum is plotted as a function of energy for various compositions. The two steps at 0.03 and 0.06 eV are due to optical phonon contributions.

sible spin gap effect on the c-axis conductivity is less pronounced in this single-layer compound than in bilayer systems as shown in the following section.

C. Temperature dependence of the electronic $\sigma_c(\omega)$

For the overdoped material with $x = 0.30$ the electronic contribution to $\sigma_c(\omega)$ allows a Drude fit to extract carrier scattering rate τ_c^{-1}.[58] The result suggests that τ_c is determined by the larger scale between ω and T. The data actually fit a general expression $\tau_c^{-1} \sim \max(\omega^\alpha, T^\alpha)$ with $1 < \alpha < 2$ using the generalized Drude formalism of Eq. (1), and τ_c^{-1} is comparable with the in-plane scattering rate τ_{ab}^{-1}.[67] This yields evidence for coherent charge transport in all the three directions.

For $x = 0.20$, it is also possible to describe σ_c formally by the generalized Drude formula with $\tau_c^{-1} \sim \omega$ at the lowest temperatures above T_c.[58] It should be noted that the generalized Drude analysis on the in-plane optical conductivity spectrum $\sigma_{ab}(\omega)$ of $x = 0.20$ is also formally possible with $\tau_{ab}^{-1} \sim \omega$ as previously discussed on 90 K Y123 which has a comparable hole density ($x \sim 0.2$) in the plane.[68,69] Although a similar relation $\tau_c^{-1} \sim \omega$ formally results from the out-of-plane optical conductivity, τ_c^{-1} is much larger than τ_{ab}^{-1}, due partly to the presence of a substantial constant (ω- and T-independent) background in τ_c^{-1}. So we cannot conclude that the charge dynamics is the same in all directions or that the charge transport is coherent in the c direction.

The electronic component of $\sigma_c(\omega)$ in the normal state for the compounds ($x \leqslant 0.16$) is nearly ω independent in the low-energy region (Figs. 4 and 6). An appreciable T dependence is not seen for $x = 0.15$, reflecting a very weak T dependence of ρ_c.[9] For $x = 0.12$, $\sigma_c(\omega)$ is gradually depressed in the energy region below $\sim$ 80 meV ($\sim$ 700 cm^{-1}), as the temperature is lowered below 200 K (see Fig. 7). This is in accordance with the semiconducting T dependence of ρ_c in the low-temperature region below $T \sim$ 200 K and seems to indicate a deepening of the pseudogap with decreasing temperature in the normal state. The depression of the optical conductivity continues through the superconducting transition, though accelerated below T_c due to the transfer of the weight to the δ function at $\omega = 0$ corresponding to the condensation of carriers into the superconducting state. Probably, the T dependence of $\sigma_c(\omega)$ would be essentially the same for $x = 0.10$, but the electronic contribution in $x = 0.10$ is too small for the present experiment to follow the T dependence of $\sigma_c(\omega)$.

Quite similar behaviors have been reported on the Y123 system.[63] The chemical hole density in the CuO_2 plane of the fully oxygenated $YBa_2Cu_3O_7$ is near $x = 0.20$ of La214, and the c-axis spectrum shows basically the same T dependence as that seen for the $x = 0.20$ compound of La214. On the other hand, $\rho_c(T)$ of oxygen-reduced compound ($T_c \sim$ 60 K) with a hole density corresponding to $x = 0.15$ or less is semiconducting below 300 K which nearly coincides with the characteristic temperature T^* in $\rho_{ab}(T)$. The σ_c spectrum of this compound clearly shows a pseudogap behavior upon reducing temperature. A possible and exotic explanation may be that based on the picture of spin-charge separation which argues that the pseudogap corresponds to a gap in the spin excitation. Since the charge transport in the c direction requires a spinon-holon recombination in this picture, the c-axis conductivity is proportional to the spinon density of states. The presence of a spin gap in oxygen-reduced or underdoped Y123 is strongly suggested by NMR (Refs. 43,44) and neutron experiments,[45,46] and actually a correlation is found between the onset of semiconducting $\rho_c(T)$ and the opening of the spin gap.[53] Note that the T dependence of ρ_c in both La214 and Y123 systems shows basically the same evolution with doping, though ρ_c values differ by an order of magnitude. The semiconducting $\rho_c(T)$ and the T dependence of the c-axis spectrum of the underdoped La214, though less pronounced as compared with those observed for 60 K Y123, are suggestive of a common mechanism working in both systems. However, the spin excitation spectrum of La214 is apparently different[70,71] and the existence of spin gap is not well established experimentally; so further detailed studies are necessary for this system.

D. Sum rule and anisotropy

Along the line of the analysis on the in-plane spectrum[10] the integrated spectral weight $N^c_{\rm eff}(\omega) = (2mV/\pi e^2)\int_0^\omega \sigma_c^{(e)}(\omega')d\omega'$ is estimated, where $\sigma_c^{(e)}$ is obtained from $\sigma_c(\omega)$ by subtracting the optical phonon contri-

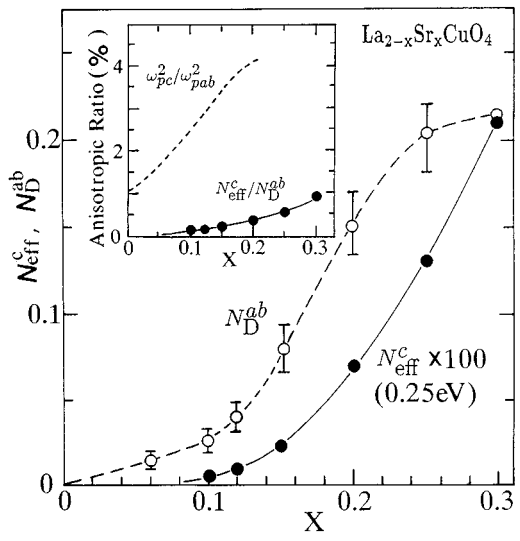

FIG. 9. $N_{\rm eff}^c$ at 0.25 eV plotted as a function of x. For comparison, the x dependence of the effective electron number for an in-plane conductivity sum at $\sim$ 0.2 eV (open circle) is shown, which is presumed to represent the Drude weight alone. The value of $N_{\rm eff}^c$ is multiplied by a factor of 10.[2] The anisotropic ratio $N_{\rm eff}^c/N_D^{ab}$ as well as the result of the band theoretical calculation (Ref. 72) in terms of the squared plasma frequency $\omega_{pc}^2/\omega_{pab}^2$ is shown in the inset.

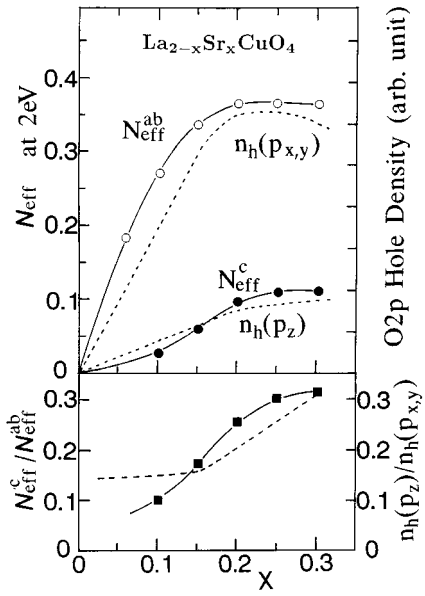

FIG. 10. x dependence of the c axis ($N_{\rm eff}^c$) and in-plane conductivity sum ($N_{\rm eff}^{ab}$) at 2.0 eV which roughly approximate the transferred spectral weight into the low-energy region of the optical conductivity spectrum with doping. For comparison, x dependences of the transferred spectral weights in the one-particle XAS [$n_h(p_{x,y})$ and $n_h(p_z)$] are indicated by the dashed curves (from Ref. 57). The anisotropic ratios $N_{\rm eff}^c/N_{\rm eff}^{ab}$ and $n_h(p_z)/n_h(p_{x,y})$, are displayed in the lower panel.

butions. The integrated $\sigma_c(\omega)$ is plotted in Fig. 8 as a function of ω. The almost discontinuous jumps at two energies correspond to optical phonons, and the magnitude of the jump gives the phonon oscillator strength. The phonon contributions are thus unambiguously subtracted to yield a purely electronic $N_{\rm eff}^c$. Because of a dip at $\sim$ 0.25 eV in the $\sigma_c(\omega)$ spectrum, $N_{\rm eff}^c$ at 0.25 eV ($\sim$ 2000 cm^{-1}) well approximates the spectral weight of the out-of-plane low-energy electronic excitations.

We plot in Fig. 9 $N_{\rm eff}^c$ at 0.25 eV as a function of x and compare it with the Drude weight N_D^{ab} which is deduced from the two-component analysis on $\sigma_{ab}(\omega)$. While N_D^{ab} linearly or quadratically increases upon doping $N_{\rm eff}^c$ remains very small and becomes appreciable only for $x>0.15$. The variation of $N_{\rm eff}^c$ is strongly superlinear with x ($N_{\rm eff}^c$ varies almost exponentially with x) in contrast to N_D^{ab} which is linear in x, and as a consequence, the anisotropic ratio ($N_{\rm D}^{ab}/N_{\rm eff}^c$) is extremely enhanced with decreasing x. For a comparison with the band theoretical calculation, we show in the inset the values of $\omega_{pab}^2/\omega_{pc}^2$, ω_{pab}^2, and ω_{pc}^2, being the in-plane and out-of-plane plasma frequencies of conduction electrons, respectively, estimated from the result of the band calculation for $La_{2-x}Sr_xCuO_4$.[72] The values of $\omega_{pab}^2/\omega_{pc}^2$ ($\sim$ 28 for $x=0.15$) are by orders of magnitude smaller than the experimental values of $N_D^{ab}/N_{\rm eff}^c$ [by definition ω_{pab}^2 (ω_{pc}^2) should be $4\pi e^2 N_D^{ab}$ ($4\pi e^2 N_{\rm eff}^c$)] and depend weakly on x.

It would be of significance to compare the spectral weight $N_{\rm eff}^c$ also with the result of polarized x-ray absorption spectroscopy (XAS).[56,57] The $a(b)$-axis polarized XAS from the core O 1s level has revealed that the weight associated with the absorption from O 1s to Cu 3d upper Hubbard band (hybridized with O 2p states) is rapidly transferred with doping to the lower-energy region, within 2–3 eV above the Fermi level, and that the transferred weight increases linearly with x up to $x\sim0.15$. This indicates that the doped holes make unoccupied states with O $2p_{x,y}$ character available for XAS from the O 1s core level.

The c-axis-polarized O 1s XAS evolves similarly with doping, though the spectral intensities corresponding to the transitions to the upper Hubbard band and to doping-induced states are weaker. This is because the doped holes have predominantly in-plane character (O $2p_z$ and Cu $3d_{x^2-y^2}$). The transferred weight in the c-axis XAS increases linearly with x up to $x=0.20$ as that in the in-plane XAS does. The ratio of the transferred weights in the two polarizations yields the ratio of the number of O $2p_z$ holes to the number of O $2p_{x,y}$ holes, $n_h(p_z)/n_h(p_{x,y})$ (Fig. 10). The ratio is nearly constant ($\sim$ 15%) up to $x\sim0.15$, and then increases for higher dopings [the ratio of the number of holes with Cu 3d character, $n_h(d_{z^2})/n_h(d_{x^2-y^2})$, is also constant with much smaller value ($\sim$ 2%) as estimated from the Cu 2p XAS]. Note that the anisotropic ratio $n_h(p_z)/n_h(p_{x,y})$ is comparable with the ratio $N_{\rm eff}^c/N_{\rm eff}^{ab}$ at the photon energy $\omega\sim$ 2 eV (the transferred weight in XAS extends over a few eV), though the x dependence of each quantity is different, reflecting different processes for the spectral weight transfer in the optical and the one-particle (XAS) spectrum. However, when we take the values of $N_{\rm eff}$ at lower ω (e.g., at 0.25 eV), $N_{\rm eff}^c$ and $N_{\rm eff}^c/N_D^{ab}$ become by more than an order of magnitude smaller. Therefore, a considerable amount of the weight is missing in the low-energy region of the c-axis optical spectrum of the underdoped compound.

E. Out-of-plane charge dynamics

The temperature dependence of ρ_c for $x<0.20$ is characterized by a kink at T_0 which coincides with the high-temperature tetragonal (HTT) to low-temperature orthorhombic (LTO) structural phase transition. T_0 starts out high (>500 K) and rapidly decreases to 0 K at $x\sim 0.22$ where superconductivity disappears.[28] The x dependence of T_0 is similar to that of the previously mentioned characteristic temperature T^*, though T_0 is somewhat lower than T^* at low dopings. As clearly seen in $\rho_c(T)$ for low dopings, the T coefficient of ρ_c changes sign at T_0. Thus, there is a compositional region where the charge transport is nonmetallic ($d\rho_c/dT<0$) in the c direction whereas metallic in the in-plane directions at $T<T_0$. Basically the same behavior is observed for $YBa_2Cu_3O_{6+x}$ (Fig. 15),[53,73] in which corresponding structural phase transition is not identified. Quite similar to La214, the sign of $d\rho_c/dT$ for underdoped Y123 changes from negative to positive at temperature near T^*.

The implications of these results would be as follows. First, the change of sign in $d\rho_c/dT$ is not primarily driven by the structural change but is a generic property of underdoped HTSC associated with the different high- and low-temperature charge dynamics which show a crossover at T^*.[50–53] The different charge dynamics are associated, if not all, with the change in spin dynamics.[74] Second, since ρ_c/ρ_{ab} continues to increase at low temperatures in spite of $d\rho_c/dT>0$, the charge transport is not strictly three dimensional (two dimensionality persists) in the highly doped superconducting regime. This is consistent with the analysis on the scattering time in Sec. IV C.

The observed semiconducting T dependence of ρ_c for the underdoped compounds appears to be connected with the pseudogap behavior in $\sigma_c(\omega)$. $\sigma_c(\omega)$ does not fit the overdamped Drude model and thus one cannot define a carrier scattering time for the c-axis conduction in the underdoped regime. By contrast, the in-plane infrared conductivity spectrum in the underdoped regime is characterized by a sharp Drude peak and a well-separated mid-IR band. The contrasting optical conductivity spectrum indicates a totally different charge dynamics in the c direction. The semiconducting dc resistivity in the c direction, while metallic in the plane, is a consequence of different charge dynamics.

The out-of-plane charge dynamics in high-T_c cuprates has been addressed from several theoretical viewpoints. One is based on the picture of non-Fermi liquid. According to, for example, the RVB scenario with spin-charge separation, a spinon and a holon have to recombine to form a physical electron which hops between planes.[75] The results of the gauge-field theory of the uniform RVB state[76] are in overall agreement with the experimental results of R_H and thermopower in both directions.[58] The gauge-field theory explains $\sigma_c(\omega)$ as follows. Owing to the bosonic distribution of the holon momentum, the motion of the physical electrons between planes is strongly diffusive, so that the c-axis optical conductivity shows a broad continuum, instead of a sharp peak at $\omega = 0$. The integrated spectral weight $N_{\rm eff}^c$ is then proportional to the holon density x (as well as the spinon density of states). In order to explain the observed strong x dependence of $N_{\rm eff}^c$, the theory has to assume the presence of a spin gap (a gap in the spinon density of states).[76,77] A problem with the gauge-field theory is that the spin gap should collapse due to the fluctuations of the gauge field. In order to stabilize the state with a spin gap in the framework of non-Fermi-liquid theories, the coupling between spins and phonons (spin-Peierls distortions) (Ref. 78) or the coupling between adjacent layers[79] has to be incorporated. This issue is still under debate in both theoretical and experimental studies.

An alternative viewpoint, based on a highly anisotropic Fermi liquid, incorporates interplanar static disorder and/or dynamical one due to, e.g., phonons which assists the hopping between planes.[80–82] In this case the interplane charge transport is determined by a competition between coherent Bloch wave propagation via the interplane hopping matrix element (t_c) and the interplane diffusion originating from random (incoherent) interplane scattering. The former process gives a Drude term and the latter an ω-independent background, and both processes are additive in σ_c. For $La_{2-x}Sr_xCuO_4$ the background term will overweigh the Drude term in the underdoped regime. As a result, σ_c is essentially ω independent and the dc resistivity ρ_c decreases with T due to the dynamical interplane scattering. Both terms are assumed to increase with doping, as the interplanar disorder increases (suppose $La_{2-x}Sr_xCuO_4$) and t_c would be enhanced due to reduced Coulomb interaction. If the t_c term dominates for the overdoped compounds, then the metallic (coherent) charge transport will result just as observed for overdoped La214. However, it should be clarified how t_c is renormalized with doping and whether this picture can explain the observed strong x dependence of $N_{\rm eff}^c$.

Nyhus *et al.*[83] have proposed that for Y123 dynamical modulation of the in-plane Cu(2)-apex-O(4) bond length by c-axis phonons may contribute to assisted interbilayer hopping and the decrease in the Cu(2)-O(4) bond length may cause a rapid increase in t_c (interbilayer hopping rate) with increase of doping. Roughly exponential doping dependences of ρ_c and $N_{\rm eff}^c$ at 0.2 eV, which are observed also for Y123, are interpreted as a consequence of strong renormalization of t_c. They suggest that t_c approximately follows $t_c\sim\exp[-\alpha w(x)]$, where α is a constant and $w(x)$ is an effective barrier width that varies linearly with doping due to the systematic decrease of the Cu(2)-O(4) bond length. A role of the O(4) phonon in the interlayer scattering has been illustrated by the c-axis-polarized Raman scattering [in the (z, z) configuration] for Y123, and in addition a strong redistribution of the c-axis phonon strengths has been reported by the infrared optical experiment.[83] However, it is not clear whether the same explanation can be applied to other systems. For example, the apical oxygen does not directly bridge the Cu atoms in adjacent layers in La214.

Concerning the dc resistivity, ρ_c may either increase or decrease with T in the highly anisotropic Fermi liquid depending on the degree of disorder and the magnitude of t_c which is set by the hole density in the plane. Even when ρ_c is increasing toward T_c, it would eventually decrease at low temperatures below T_c if not masked by the superconducting transition. This is a critical difference from the non-Fermi-liquid theories[75,76,84] which predict that a positive T coefficient ($d\rho_c/dT>0$) will be observed at sufficient high temperatures and that ρ_c would continue to increase toward

infinity as T is decreased below T_c. Such an argument is, of course, academic, but there is an experimental fact that ρ_c continues to increase when superconductivity is suppressed by applying magnetic field or by substituting Cu with Zn.[85]

Other than these two, various models for the anomalous c-axis transport have been proposed, including anisotropic localization with t_c renormalized by impurity scattering,[86] dynamical dephasing process,[87] and one incorporating an effect of superconducting fluctuations.[88] A critical check is necessary if any of these models can explain all the unusual features of the c-axis charge dynamics presented here.

V. OPTICAL RESPONSE IN THE HIGH-T_c SUPERCONDUCTING STATE

A. Brief review of the in-plane superconducting response

The superconducting energy gap (2Δ) and superfluid density (or spectral weight of superconducting condensate) are two basic parameters which characterize superconducting state for any type of superconductivity, and thus are expected to be relevant to the infrared optical response of the high-T_c superconductors (HTSC's). As Tanner and Timusk reviewed,[20] the in-plane infrared spectra of HTSC's in the superconducting state is still puzzling. In most cuprates an onset of absorption, corresponding to 2Δ in ordinary superconductors, is seen between 300 and 600 cm^{-1} (100 cm^{-1} = 12.4 meV). However, there is no correlation between the onset and T_c.

If there is a true superconducting gap, the reflectivity should be unity up to 2Δ. In the high-T_c materials the 100% reflectance has not been confirmed so far. The experimental results of Kramers-Kronig- (KK) transformed optical conductivity lose their accuracy below $\sim$ 200 cm^{-1}, and it is far from clear if there is a true gap at lower frequencies below 200 cm^{-1}, where the accuracy of the result is poor. Furthermore, it is also possible to interpret the lowest-temperature spectrum as that dominated by the mid-IR band which is not missing below T_c.

Even below 200 cm^{-1} direct absorption measurements,[89,90] which yields much more accurate data, find for $YBa_2Cu_3O_7$ that the absorptivity, $1-R$, is finite and rises toward lower frequencies. So it appears that there is no true gap seen even in the in-plane optical spectrum of this most perfect and stoichiometric crystal among the various high-T_c cuprates.

Even though we cannot say anything definite about the gap, the amount of conductivity that condenses into the δ function at $\omega = 0$ is given less ambiguously from the missing area of the optical conductivity spectrum in the superconducting state. The missing area should be equal to $\omega_{ps}^2/8$ by the sum rule argument with ω_{ps} being the plasma frequency of superconducting carriers. ω_{ps} is related to the superfluid density (n_s) and the effective mass of the condensed carriers m^* by $\omega_{ps}^2 = 4\pi n_s e^2/m^*$, and also to the London penetration depth (λ_{ab}) by $\lambda_{ab} = 1/2\pi\omega_{ps}$ with ω_{ps} in cm^{-1}. For various cuprates the values of λ_{ab} as well as its temperature dependence below T_c are in fairly good agreement with those determined by other techniques such as μSR.[91,92]

The most significant finding about the superfluid density is that for the underdoped materials the values of ω_{ps}^2 increase roughly proportionally to the chemical hole density δ defined by formal valence of Cu, $Cu^{2+\delta}$. As is well known from the μSR studies,[91] $\omega_{ps}^2(\lambda_{ab}^{-2})$ shows a linear dependence on T_c for various materials in the underdoped region. Thus, it follows that $T_c \sim \delta$ which is suggestive of boson condensation. Furthermore, it is suggested that ω_{ps}^2 roughly coincides with the spectral weight of a Drude component in the normal-state optical conductivity spectrum when analyzed based on the two-component model.[20] This is roughly the case with the materials near optimal doping, and thus in agreement with the superconductivity in the clean limit in that a superconducting gap is larger in comparison to the width of the Drude spectrum so that most of the free carriers condense into the superconducting state.

At higher doping ω_{ps} no longer increases but saturates and then decreases as doping proceeds. At higher doping ω_{ps} no longer increases but saturates and then decreases with further. The decrease in ω_{ps} is evidenced by the μSR experiments on overdoped $Tl_2Ba_2CuO_{6+y}$.[93,94] Although a systematic study of the in-plane optical spectrum has yet been completed in the overdoped superconducting region, a possible explanation will be given in the next based on the results of the c-axis spectrum.

B. Anomalous c-axis optical response (Josephson plasma)

We have described above why the optical experiment, one of the standard techniques, has yielded no definitive evidence for a superconducting gap in HTSC's. Fortunately, the problems with the in-plane optical spectrum in the superconducting state are less serious in the out-of-plane spectrum. So one can unambiguously explore the evolution of the superconducting optical response with doping.

The c-axis reflectivity spectrum in the normal state of the compounds with $x \leqslant 0.16$ looks like that for insulators. A sharp reflectivity edge was found to develop below T_c in the very-low-frequency region as if an insulator-metal transition takes place at T_c.[21] Now it has been known that the c-axis spectra of many underdoped cuprates show essentially the same spectral change at T_c.[63,65,95–98] As was clearly demonstrated for La214,[21] the reflectivity edge corresponds to the plasma edge of the superconducting condensate, not to the superconducting gap, since the edge arises from the zero of the real part of the dielectric function, $\epsilon_1(\omega) = 0$, not from $\sigma_c(\omega) = 0$. Normally, the superfluid density is as high as the carrier density in the normal state, so that the corresponding plasma edge is observed in the 1–10 eV region which is little affected by the superconducting transition.

Usually, a superconducting gap at $T << T_c$ is defined by $\sigma(\omega) = 0$ at $\omega = 2\Delta$.[99] As $\sigma = 0$ and $\epsilon_1 < 0$ for $\omega \leqslant 2\Delta$, the reflectivity is unity below 2Δ and falls down at higher frequencies. Contrary to this, the superconducting response in the present case is governed by a radical change of $\epsilon_1(\omega)$ across T_c. ϵ_1 in the normal state is positive and nearly constant in the lowest-frequency region just like for insulating dielectrics. Upon entering the superconducting state, ϵ_1 becomes a rapidly decreasing function of ω toward $\omega = 0$, and crosses zero at frequency $\omega = \omega'_{ps}$. We found that in this ω region ϵ_1 is well approximated by $\epsilon_1^s(\omega) = \epsilon_\infty - \omega_{ps}^2/\omega^2$ with $\epsilon_\infty = 25$ and $\omega_{ps}^2 = \epsilon_\infty \omega_{ps}'^2$ (Fig. 11). The frequency ω_{ps} and thus the reflectivity edge at ω'_{ps} shift to higher frequencies

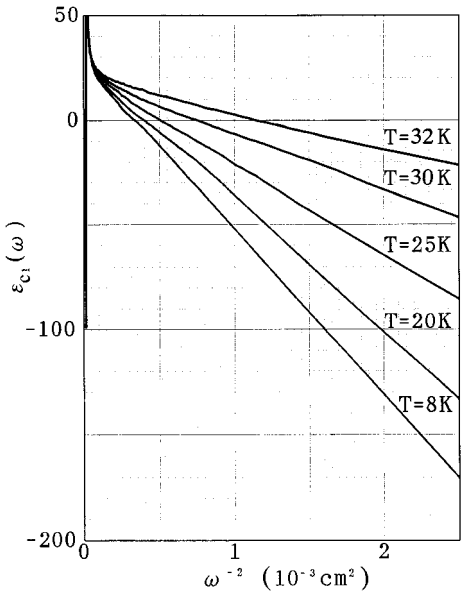

FIG. 11. Real part of dielectric function of $La_{1.85}Sr_{0.15}CuO_4$ plotted against ω^{-2}. The linear relationship between ϵ_1 and ω^{-2} is characteristic of the superconducting state, and the slope gives the value of ω_{ps}^2.

with decreasing temperature, in accordance with, e.g., the increase in the carrier density condensed in the superconducting state.

A very sharp plasma edge in the c-axis spectrum of HTSC's implies that the plasma frequency (ω_{ps}) becomes extremely low so that the plasma edge is located within the superconducting gap region. When it is located inside the gap, there is no decay channel for the superfluid plasma, which gives rise to a very sharp plasma edge. This phenomenon is reminiscent of the Josephson plasma which occurs in a weakly coupled Josephson junction.[100] As we shall describe in the next section, the observed c-axis plasma edge can be identified as that associated with a plasma in Josephson-coupled layered superconductors, i.e., Josephson plasma.[101,102] In this case the plasma frequency is primarily determined by the critical current density in the c direction.

While the low plasma frequency arises from the small density of carriers in the barrier for a single Josephson junction, the origin of the extremely low ω_{ps} can be traced back to the c-axis optical conductivity spectrum $[\sigma_c(\omega)]$ in the normal state of underdoped compounds. As demonstrated in Sec. IV, $\sigma_c(\omega)$ in the underdoped regime is extremely low in the low-energy region (below $\sim$ 2000 cm^{-1}) and is further reduced by a pseudogap below $\sim$ 700 cm^{-1}. As we see below, an appreciable suppression of σ_c in the superconducting state takes place below $\sim$ 200 cm^{-1} (the maximum energy below which σ_c is depressed below T_c extends up to $\sim$ 500 cm^{-1}), which is smaller than the width of the pseudogap in the normal state. Therefore, the spectral weight that condenses into $\delta(\omega)$ below T_c has to be very small due to the requirement of the sum-rule.

C. Gap structure and evolution of the c-axis response with temperature

The c-axis optical conductivity spectra for $x = 0.15$ with optical phonons removed are shown in Fig. 12 at temperatures just above T_c and well below T_c (T=8 K). The optical conductivity at the lowest temperature (8 K) is depressed below $\sim$ 600 cm^{-1} ($\sim 20k_BT_c$), and seems uniformly suppressed to very small values, in the low-frequency region (below $\sim$ 200 cm^{-1}). The spectral shape looks like that for a BCS superconductor in the dirty limit with a gap of about 200 cm^{-1} ($\sim 7k_BT_c$).

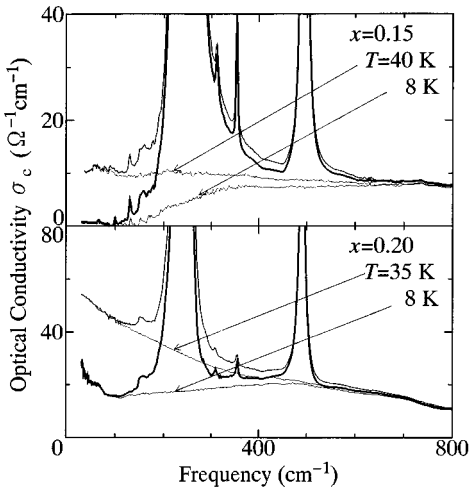

FIG. 12. c-axis optical conductivity spectra with phonons removed (thin lines) for $x = 0.15$ and 0.20 in the normal state (just above T_c) and in the superconducting state (T = 8 K, well below T_c).

We have described in the previous section that the dielectric function $\epsilon_1^s(\omega)$, which corresponds to the one postulated by the London model of a clean-limit BCS superconductor, approximates the low-temperature spectrum. On the other hand, the low-temperature $\sigma_c(\omega)$ looks like one expected for a dirty-limit BCS superconductor. The apparent contradiction arises from the fact that $\sigma_c(\omega)$ is suppressed up to much higher frequencies than the position of the plasma edge where $\epsilon_1(\omega) = 0$. Another controversy is that the high-T_c superconductor seen from the in-plane optical conductivity is the one in the clean limit, while it seems in the dirty limit from the c-axis optical conductivity. This is possible for a Josephson-coupled array of superconducting layers in the clean limit stacked in the c direction.[103]

As σ_c in the normal state is nearly flat and is suppressed uniformly below $\sim$ 200 cm^{-1} in the superconducting state, the missing area in $\sigma_c(\omega)$ which should go into a δ function at $\omega = 0$ can be approximated at $T << T_c$ by the area of a rectangle with the height ρ_c^{-1} (ρ_c is the dc resistivity just above T_c) and the width given by an apparent superconducting gap width ($2\Delta \sim$ 200 cm^{-1}). So the missing area ($=\frac{1}{8}\omega_{ps}^2$) is roughly equal to $\rho_c^{-1}2\Delta/\hbar$. This implies that the out-of-plane magnetic penetration depth (c-axis London length) λ_c ($=1/2\pi\omega_{ps}$ with ω_{ps} in cm^{-1}) scales as $\lambda_c^{-2} \sim \rho_c^{-1}2\Delta$. We shall see that λ_c actually shows a rapid increase with reducing x just following the rapid increase in ρ_c (Fig. 16 and see also Ref. 64).

For a Josephson-coupled layered superconductor λ_c is related to the Josephson critical current density J_c by $J_c = c\Phi_0/8\pi^2\lambda_c^2 s$, where Φ_0 is the flux quantum and s is the interlayer spacing.[104] The critical current density at $T=0$ is

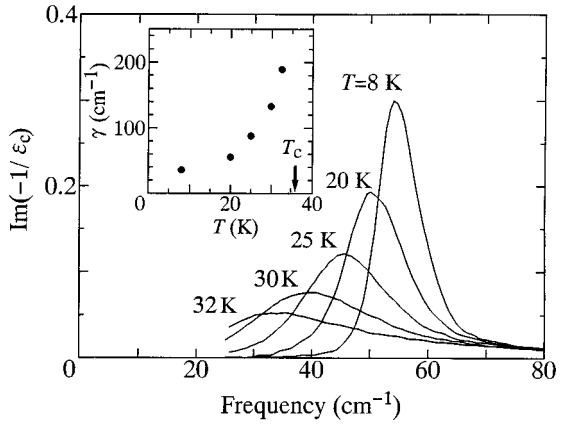

FIG. 13. Energy loss function, Im $[-1/\epsilon(\omega)]$, for $La_{1.85}Sr_{0.15}CuO_4$. The peak appearing below T_c corresponds to the plasma reflectivity edge. The peak width γ is plotted against temperature in the inset.

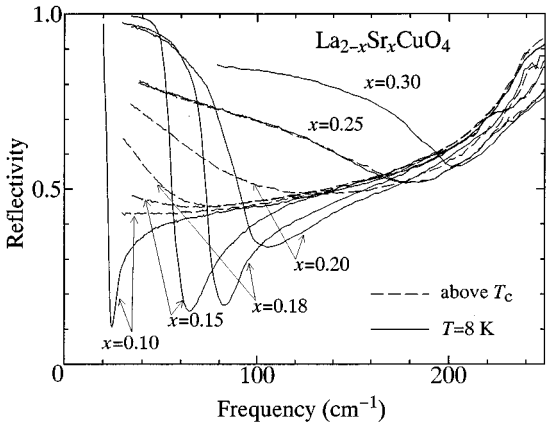

FIG. 14. c-axis-polarized infrared reflectivity spectra above ($T\sim$ 40 K, dashed curve) and below T_c (T = 8 K, solid curve) for various compositions between 0.10 and 0.30. The data at two temperatures (T = 8 and 40 K) for x = 0.25 and 0.30 almost coincide, giving evidence for the absence of bulk superconductivity in the overdoped regime.

given by $J_c=\pi\Delta/2e\rho_n s$ with ρ_n, the normal-state resistivity. If we assume $\rho_n=\rho_c(T_c)$, this relation leads to $\lambda_c^{-2}=(2\pi^2/\hbar c^2)\rho_c^{-1}2\Delta$ which is exactly what we estimate for λ_c from the c-axis optical spectrum. This, together with the x dependence of λ_c, gives evidence that the c-axis optical response is determined by the Josephson plasma and thus HTSC is regarded as an alternating stack of superconducting CuO_2 planes and insulating building blocks (such as La_2O_2 layers) at least in the underdoped regime. The Josephson coupling between the planes reconfirms the assumption that the pairs are formed within the plane.

Given these materials, one could, in principle, discuss the gap structure or the pairing symmetry of HTSC under the assumption that the pairs are formed within a CuO_2 plane and thus there is only one energy scale in the superconducting state. However, the experimental results are puzzling and confusing. Some results favor fully gapped superconductivity (s-wave gap) but others favor gapless superconductivity such as the one with gap function having nodes in **k** space (e.g., d-wave gap). The results that favor an s-wave gap are (i) the spectral shape of $\sigma_c(\omega)$ at $T<<T_c$ and (ii) the temperature dependence of $\omega_{ps}^2(\lambda_c^{-2})$. The experimental data for $x=0.15$ appear to fit better to the two-fluid or s-wave Ambegaokar-Baratoff model.[21] Shibauchi *et al.*[105] also demonstrated that $\lambda_c(T)$ for x = 0.15 determined by the microwave measurement is consistent with the s-wave T dependence of Δ assumed for a Josephson-coupled array of superconducting layers.

On the other hand, the results that favor a d-wave gap are (iii) the evolution of $\sigma_c(\omega)$ with T and (iv) the Zn-doping effect. As temperature rises, the depressed region is filled up rather uniformly, but an appreciable decrease in the gap width is not seen with an increase of T, which should be observed for a BCS dirty-limit superconductor. The increased $\sigma_c^s(\omega)$ in the gap region is responsible for the increasing damping of the plasma edge at higher temperatures. Figure 13 demonstrates the loss function Im $[-1/\epsilon(\omega)]$ calculated via the KK transformation. The loss function shows a well-defined peak at $\omega\sim\omega_{ps}'$ and the rapid increase of the peak width with T indicates a rapid increase of the damping of the plasma. The increase of $\sigma_c^S(\omega)$ and the concomitant increase in the damping are suggestive of the gapless nature of superconductivity.

The Zn-doping effect on the superconducting spectrum would be useful for discriminating the pairing symmetry.[106] Zn substituted for Cu in the plane is a strong scatterer of the carriers and radically reduces T_c. A preliminary result of $\sigma_c(\omega)$ for $La_{1.85}Sr_{0.15}Cu_{1-z}Zn_zO_4$ indicates that Zn does not reduce the magnitude of the gap, but fills in the gap region,[85] apparently consistent with the pairing-state gap nodes.

D. Evolution of the *c*-axis response with doping

An issue that follows is what happens as doping proceeds. Reflectivity spectra at the lowest temperature ($\sim$ 8 K) and just above T_c are shown in Fig. 14, for various compositions of La214 in the range $0.10\leqslant x\leqslant 0.30$. The superfluid plasma edge shifts to higher frequencies with an increase of doping and remains very sharp up to $x=0.16$. However, for $x=0.18$ the edge becomes broad with a shallower dip and the low-frequency reflectivity does not reach the value close to 1 down to the lowest frequency of the experiments. Note that such a dramatic response does not take place for x = 0.25 (and x = 0.30), although a superconducting transition ($T_c\sim$ 15 K) is seen in resistivity and magnetic susceptibility measurements. This fact indicates that the superconductivity in x = 0.25 is not a bulk property, and provides a support for the presence of a boundary between superconducting and nonsuperconducting phases at $x\sim$ 0.22 in coincidence with the tetragonal-orthorhombic boundary.[28,91]

The optical conductivity $[\sigma_c(\omega)]$ spectra are shown in Fig. 15. In this figure the spectrum in the normal state just above T_c and at two temperatures below T_c, T = 8 and 25 K, are shown in order to demonstrate how much the spectral weight is missing in the superconducting state. The electronic contribution to the spectrum for $x\leqslant 0.16$ is consider-

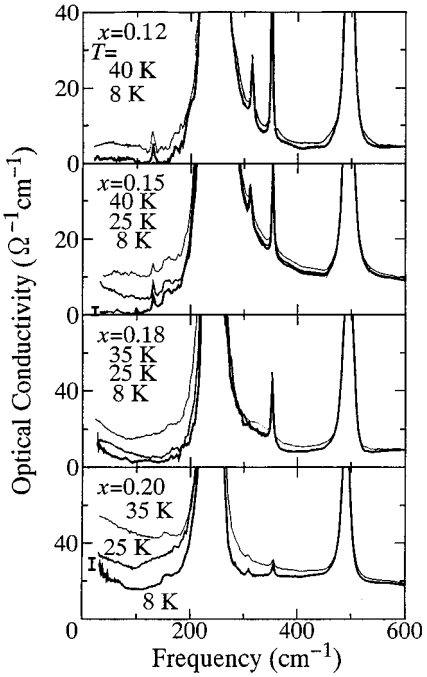

FIG. 15. c-axis optical conductivity spectra above ($T = 35$ or 40 K, thin solid curve) and below T_c ($T = 25$ and 8 K, thick solid curves) for four compositions in the superconducting phase.

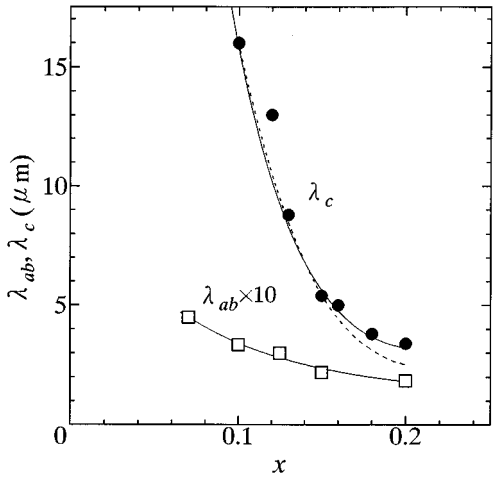

FIG. 16. The $T \rightarrow 0$ value of out-of-plane (λ_c) and in-plane (λ_{ab}) magnetic penetration depth plotted against x. The value of λ_c is determined from the present optical spectrum measured at 8 K (well below T_c) by estimating either missing area of $\sigma_c(\omega)$ or the slope of ϵ_1 vs ω^{-2} plot. The value of λ_{ab} is taken from μSR results in Ref. 91. The dashed curve indicates the x dependence of $\rho_c^{-1}2\Delta$ with ρ_c and 2Δ being the dc resistivity just above T_c and the approximate width of the superconducting gap ($2\Delta \sim 200$ cm^{-1}, alomst independent of x), respectively. The relatively enhanced value of λ_c (and of λ_{ab}) at $x \sim 0.12$ arises from the suppression of superconductivity near $x = 1/8$.

ably small below ~ 2000 cm^{-1} in the normal state, and $\sigma_c(\omega)$ is almost ω independent in the lowest-frequency region. The suppression continues across T_c and σ_c at 8 K becomes very small. One should note that the energy scale of the superconducting state, a maximum energy of the σ_c depression below T_c, is ~ 500 cm^{-1} which amounts to 17 $k_B T_c$ or more and seems not dependent on x nor correlated with the T_c magnitude. The plasma edge is located in this gap region which is the reason for the very small damping. Though σ_c is uniformly suppressed over a fairly wide frequency region, a tiny σ_c remains even at $T \ll T_c$. Therefore, strictly speaking, there is no definite gap in the superconducting state. It might be possible that the residual conductivity is extrinsic in origin, such as that arising from inhomogeneous distributions of Sr composition in a crystal. There is some magnetic phase in the vicinity of $x = 0.12$.[107] The magnetic phase is probably similar to that clearly identified for $La_{2-x}Ba_xCuO_4$ with $x = 0.125$ where an antiferromagnetic order is observed at low temperatures, accompanied with the tetragonal phase transition at ~ 60 K.[108,109] A recent μSR study has confirmed an AF order occurring near $x = 0.12$ also in $La_{2-x}Sr_xCuO_4$ resulting in a suppression of superconductivity.[115] Actually, the plasma edge for our crystal with $x = 0.12$ is located at relatively low frequency (and correspondingly the out-of-plane magnetic penetration depth is enhanced as we shall see in Fig. 16), indicating a suppression of superconductivity to some extent. This magnetic phase would be mixed up slightly in a crystal with x near 0.12 due to compositional fluctuation and would likely behave as magnetic impurities. Gapless superconductivity induced by magnetic impurities was suggested by the inelastic neutron scattering experiment on a La214 single crystal with $x \sim 0.14$.[110]

The onset of superconductivity for the highly doped compounds ($x = 0.18$ and 0.20) is signaled by the depression of $\sigma_c(\omega)$ below ~ 500 cm^{-1}. In the optical conductivity spectrum a considerable conductivity remains at $T = 8$ K, filling up the entire low-frequency region and even increasing toward $\omega = 0$. This is responsible for the appreciable damping of the superfluid plasma. The Drude-like residual conductivity near $\omega = 0$, which cannot be attributed to quasiparticle excitations, is the reason for the reflectivity significantly lower than unity at the lowest frequencies.

Since the crystal with $x = 0.20$ is near the phase boundary at $x \sim 0.22$, some portion of the crystal might be a nonsuperconducting metal (tetragonal phase) which might be responsible for the Drude-like residual conductivity. As a rough estimate, the weight of the residual conductivity at 8 K occupies 10% and 25% of the missing (condensed) spectral weight for $x = 0.18$ and 0.20, respectively. Such a strongly gapless spectrum is rather suggestive of the presence of an appreciable density of normal carriers in the superconducting state.[111]

These two types of superconducting spectra depending on the doping level are also observed in bilayer systems, $YBa_2Cu_3O_{6+x}$ (Refs. 63,112) and $Pb_2Sr_2(Y,Ca)Cu_3O_8$.[65] The σ_c spectrum of $T_c = 60$ K Y123 which is in the underdoped regime is essentially the same as that observed for La214 with $x \leq 0.16$. Surprisingly, fully oxygenated Y123 ($T_c = 90$ K) shows a strongly gapless spectrum just like that of La214 with $x = 0.20$. Similar spectra between single-layer and bilayer systems indicate that the properties are determined primarily by the doped hole density in the CuO_2 plane. Another important point is that the superconducting spectrum has a strongly gapless feature even for

$YBa_2Cu_3O_7$ which is the most stoichiometric and perfect crystal among the known high-T_c materials.[111] Therefore, such a gapless spectrum appears to be inherent to highly doped cuprates.

In the highly doped regime, the in-plane spectrum of the fully oxygenated Y123, which was measured by the direct absorptivity[89,90] and hence is much more accurate than those determined by the infrared reflectivity measurements, shows a very similar gapless feature with a Drude-like peak at $\omega = 0$ remained even at 4.2 K. The increase in the residual conductivity in the optical conductivity spectrum, perhaps corresponding to the increase in normal carrier density, is connected to the saturation and subsequent increase of λ_{ab} (in-plane London penetration depth) observed in the μSR experiments in the highly and overdoped regime.[93,94,113] We see below a similar trend in λ_c in the highly doped region. Basically the same feature observed in the superconducting spectra for both polarizations and for any doping reconfirms that the anisotropic gap does not make sense and the pairing occurs predominantly within the CuO_2 plane.

The estimated λ_c is plotted in Fig. 16 as a function of x. The value of λ_c for $x = 0.15$ is 5.5 μm and is 22 times longer than the in-plane length $\lambda_{ab}=0.25$ μm.[91,92] The anisotropy in λ, in terms of the anisotropy in the effective mass, $m_c/m_{ab} = \lambda_c^2/\lambda_{ab}^2 \sim 500$ which is much larger than the band theoretical prediction $m_c/m_{ab} \sim 28$ for $x = 0.15$ (but is comparable with $N_D^{ab}/N_{\rm eff}^c$ estimated in Sec. IV D). The x dependence of λ_c is quite distinct from that of the in-plane London length (λ_{ab}) determined by μSR which shows a much slower change in the underdoped regime. The x dependence of λ_{ab}^2 should arise from the x dependence of the superfluid density n_s assuming that m_{ab}^* is not strongly dependent on x. On the other hand, the x dependence of λ_c is controlled by the coupling strength between the superconducting CuO_2 planes, namely, by the c-axis Josephson critical current density J_c as remarked in the preceding section. J_c turns out to be inversely proportional to the c-axis resistivity ρ_c which is determined by the electronic state in the CuO_2 plane, not in the barriers (insulating layers) between the CuO_2 planes. Here, one should note that ρ_c shows a semiconducting temperature dependence in most underdoped cuprates and that the c-axis Josephson plasma frequency (or J_c) is determined by the value of ρ_c at T_c (just above T_c). Indeed, the anisotropy in the superconducting state, $\lambda_c^2/\lambda_{ab}^2$, is nearly identical to the resistivity anisotropy ρ_c/ρ_{ab} at $T=T_c$. This indicates in some sense that the interlayer (Josephson) coupling is determined by at which temperature the superconductivity sets on, or conversely T_c, and thus superconductivity may be controlled by the interlayer coupling.[114]

In the highly doped region both λ_c and λ_{ab} show a tendency for saturation.[91] Now that we have seen the strongly gapless spectrum, we understand the reason for the saturation. The residual conductivities in the superconducting state, which are observed also in the in-plane spectrum of $YBa_2Cu_3O_7$ (Refs. 89,90 and may arise from the presence of normal carriers, increase with doping and compensate the increase in σ_c in the normal state. For still higher dopings λ_c would increase again [the turnover of λ_{ab} is widely known from μSR experiments on $Tl_2Ba_2CuO_{6+y}$ (Refs. 93,94)]. One can easily deduce that the residual σ_c would overcompensate the increase in the normal-state σ_c.

The strongly gapless spectrum of highly doped material seems to be a d-wave superconductor with appreciable density of normal impurities. Since a quite similar spectrum is observed for the most stoichiometric compound $YBa_2Cu_3O_7$,[111] the presence of normal impurities of high density is unlikely. The result is rather suggestive of the presence of normal carriers. The density of normal carriers rapidly increases with doping. The presence of normal carriers may signal a phase separation (into superconducting and normal metallic phase) or strong fluctuations of the amplitude of superconducting order parameter.

The crossover between these two superconducting regimes is associated with the change in the T dependence of the normal-state c-axis resistivity, from semiconducting to ''metallic.'' The T dependence of ρ_c in the highly doped region is not necessarily the same as that of the in-plane resistivity and the resistivity anisotropy ρ_c/ρ_{ab} increases with lowering temperature. It seems possible to speculate that the normal carriers present in the superconducting state originate from the overdoped metallic phase which is mixed in the superconducting phase in the highly doped compounds and is responsible for the apparent metallic $\rho_c(T)$ in the normal state.

VI. CONCLUSIONS

We have presented the c-axis optical spectrum and its evolution with doping in the $La_{2-x}Sr_xCuO_4$ system. Together with the results of the in-plane spectrum we published previously, we have got now an almost complete set of data for this prototypical high-T_c system. The implications of the results of the c-axis optical spectrum go well beyond the evidence for a strongly anisotropic electronic state of the cuprates. Highlights are the completely different charge dynamics in the c direction and the anomalous c-axis optical response in the superconducting state, particularly in the underdoped regime. They are quite generic and characteristic of the electronic state of HTSC. We suggest that the highly doped superconducting regime is a crossover region from the underdoped to the overdoped regime where the charge transport is coherent in all directions and the superconducting disappears. The c-axis optical and transport properties of the highly doped compounds seem to be something like a mixture of those in the two regimes.

However, we are still at some distance from complete understanding of the electronic state in HTSC. In order to achieve the complete understanding we have to wait for a much more complete set of data for the evolution of the spin excitation spectrum with doping which enables a detailed comparison between charge and spin dynamics. Below we summarize the c-axis optical properties in the normal and superconducting states of HTSC.

A. Optical spectrum in the normal state

The in-plane optical conductivity for the same dopant concentration is nearly material independent both in magnitude and ω dependence. By contrast, the magnitude of the

c-axis optical conductivity as well as the c-axis dc resistivity is strongly material dependent, that is, dependent on the species of the building blocks in between the CuO_2 planes. However, what is common with all the materials is the strong doping dependence of the c-axis resistivity and optical conductivity. Upon doping holes a transfer of the spectral weight takes place in the out-of-plane spectrum from high-energy region (5–6 eV) to low-energy region (below 3 eV). This is basically parallel to the evolution of the in-plane spectrum. In the case of the in-plane spectrum, the transferred weight forms a Drude peak at $\omega = 0$ together with a mid-IR band. Both bands rapidly develop and the mid-IR band which dominates in the underdoped regime softens as doping proceeds. By contrast, in the case of the c-axis spectrum the transferred weight forms a band peaked at high energy, ~ 2 eV, which does not show an appreciable softening with an increase of doping, though the total weight increases. As a consequence of this ''pinning'' of the transferred spectral weight, the low-energy spectral weight is quite small, much smaller than that expected from the band calculations. In the underdoped regime, the conductivity is well below the minimum value for metallic conduction and is spread over a wide energy range instead of forming a Drude peak at $\omega = 0$. This is evidence for an incoherent charge transport in the c-axis direction arising from purely electronic interactions, not from disorder or phonon effects.

The suppression is rapidly released, and the c-axis conductivity eventually forms a Drude peak at $\omega = 0$ in the overdoped regime. In conjunction with this, the anisotropy in transport properties is rapidly reduced with increasing dopant concentration. This is a general properties among the known high-T_c cuprates, independent of the species of the building blocks.

Restricted to the underdoped regime, the most surprising and characteristic feature of $\sigma_c(\omega)$ is a pseudogap behavior in that the conductivity below ~ 0.08 eV is further reduced with lowering the temperature from above T_c. The semiconducting c-axis resistivity is connected with this pseudogap behavior. The observed pseudogap cannot be attributed to a conventional semiconducting gap in the charge excitation spectrum, since no gap feature is seen in the in-plane spectrum which is dominated by a sharp Drude peak. This is strong evidence for totally different charge dynamics in the c direction, as also highlighted by the peculiar sign and T dependences of the Hall and Seebeck coefficients. A more pronounced pseudogap is observed for the underdoped Y123 in which it is obviously connected with the ''spin gap'' observed in the magnetic measurements. In the case of La214, the correlation between the pseudogap in $\sigma_c(\omega)$ and the magnetic response is not so clear, but the characteristic temperatures in the c-axis charge transport and the magnetic susceptibility in the underdoped regime are comparable, starting out high ($\sim$ 500 K) at low dopings and dropping rapidly with an increase of x.

B. Optical response in the superconducting state

Even at the moment we cannot say anything definitively about the superconducting gap from the results of the in-plane optical spectra.[14] This is because there are problems with the accuracy of measurements which arise from the ambiguity in the low-frequency extrapolation in the Kramers-Kronig analysis and from the complications whether the mid-IR band is present or not in the in-plane spectrum.

Some of the ambiguity with the in-plane spectrum has been resolved by the measurements of the c-axis optical response. Since the c-axis spectral weight of the superconducting condensate is extremely small owing to the normal-state σ_c severely suppressed over a wide energy range, two dimensionality in the electronic state persists into the superconducting state. As a consequence the superconducting pairs are likely formed within the plane, and we expect that the c-axis optical response is also controlled by an in-plane superconducting gap.

The c-axis reflectivity spectrum of underdoped material is found to show an extraordinary response in the superconducting state. Below T_c a sharp plasma edge shows up in the very-low-frequency region. This can be identified as a Josephson plasma mode in Josephson-coupled layered superconductors. Due to weak coupling between the layers, the strength of which is determined by the c-axis resistivity at T_c, the plasma edge appears within the superconducting gap ($\sim$ 200 cm^{-1} in width). The extremely low plasma frequency originates from the suppressed spectral weight in the normal state.

Since the Josephson plasma suffers damping only by excitations across a superconducting gap at very low temperatures ($T << T_c$), the evolution of the c-axis Josephson plasma with doping is closely connected to the development of the superconducting gap or in-gap states with doping. The experimental results on $La_{2-x}Sr_xCuO_4$ indicate that the c-axis optical conductivity spectrum is gapless at any doping. The gaplessness may be consistent with the results of various other experiments, many of which suggest d-wave pairing in HTSC. However, the c-axis spectrum in the low-doping regime ($x \leq 0.16$) is only weakly gapless and σ_c is uniformly suppressed in the low-frequency region like that in a BCS s-wave superconductor in the dirty limit, so that the damping of the plasma is very small. Note that the width of the gap, the frequency region where σ_c is uniformly suppressed, does not appreciably decrease with a decrease of x (or T_c). This suggests that the phase fluctuations of the superconducting order parameter might be important in the underdoped regime.[115]

At higher dopings ($x > 0.16$) the c-axis superconducting spectrum becomes strongly gapless with a Drude-like peak at $\omega = 0$ even at $T << T_c$, giving rise to a strongly damped Josephson plasma. Such a gapless spectrum is suggestive of the presence of a substantial density of normal fluid, perhaps a precursory effect of a crossover from a superconducting to a nonsuperconducting overdoped regime, or fluctuations of the amplitude of the superconducting order parameter become dominant as one approaches the overdoped regime.

ACKNOWLEDGMENTS

We would like to thank N. Nagaosa, M. Imada, and M. Tachiki for stimulating discussions. The present research is supported by a Grant-in-Aid for Scientific Research on Priority Area, ''Science of High T_c Superconductivity'' from the Ministry of Education, Science, and Culture of Japan and partly by the Mitsubishi Science Foundation.

[1] G. Travaglini and P. Wachter, Phys. Rev. B **30**, 1971 (1984).
[2] B. C. Webb, A. J. Sievers, and T. Mihalisin, Phys. Rev. Lett. **57**, 1951 (1986).
[3] S. Uchida, K. Kitazawa, and S. Tanaka, Phase Trans. **8**, 95 (1987).
[4] J. G. Bednorz and K. A. Müller, Z. Phys. B **64**, 189 (1986).
[5] S. Tajima *et al.*, Jpn. J. Appl. Phys. **26**, L432 (1987).
[6] T. Timusk and D. B. Tanner, in *Physical Properties of High Temperature Superconductors* I, edited by D. M. Ginsberg (World Scientific, Singapore, 1989), p. 339.
[7] S. E. Stupp and D. M. Ginsberg, in *Physical Properties of High Temperature Superconductors* III, edited by D. M. Ginsberg (World Scientific, Singapore, 1992), p. 2.
[8] S. L. Cooper *et al.*, Phys. Rev. B **41**, 11 605 (1990).
[9] I. Terasaki *et al.*, Physica C **165**, 152 (1990).
[10] S. Uchida *et al.*, Phys. Rev. B **43**, 7942 (1991).
[11] S. L. Cooper *et al.*, Phys. Rev. B **45**, 2549 (1992).
[12] T. Arima, Y. Tokura, and S. Uchida, Phys. Rev. B **48**, 6597 (1993).
[13] T. Ito, H. Takagi, T. Ido, S. Ishibashi, and S. Uchida, Nature (London) **350**, 596 (1991).
[14] B. Batlogg, H. Takagi, H. L. Kao, and J. Kwo, in *Electronic Properties of High-T_c Superconductors*, edited by H. Kuzmany, M Mehring, and J. Fink (Spinger, Berlin, 1993), p. 5.
[15] W. E. Pickett, Rev. Mod. Phys. **61**, 433 (1989).
[16] Y. Iye *et al.*, Physica C **153–155**, 26 (1988).
[17] D. G. Clarke, S. P. Strong, and P. W. Anderson, Phys. Rev. Lett. **72**, 3218 (1994); P. W. Anderson (unpublished).
[18] D. A. Brawner, Z. Z. Wang, and N. P. Ong, Phys. Rev. B **40**, 9329 (1989); L. Forro *et al.*, Phys. Scr. **41**, 365 (1990).
[19] Y. Nakamura and S. Uchida, Phys. Rev. B **47**, 8369 (1993).
[20] D. B. Tanner and T. Timusk, in *Physical Properties of High Temperature Superconductors* III, edited by D. M. Ginsberg (World Scientific, Singapore, 1992), p. 363, and references therein.
[21] K. Tamasaku, Y. Nakamura, and S. Uchida, Phys. Rev. Lett. **69**, 1455 (1992).
[22] I. Tanaka and H. Kojima, Nature (London) **337**, 21 (1989).
[23] H. Takagi *et al.*, Phys. Rev. B **40**, 2254 (1989).
[24] J. B. Torrance *et al.*, Phys. Rev. B **40**, 8872 (1989).
[25] F. Gugenberger *et al.*, Phys. Rev. B **49**, 13 137 (1994).
[26] J. D. Axe *et al.*, Phys. Rev. Lett. **62**, 2751 (1989).
[27] Y. J. Uemura (private communication).
[28] H. Takagi *et al.*, Phys. Rev. Lett. **68**, 3777 (1992).
[29] G. A. Thomas *et al.*, Phys. Rev. Lett. **61**, 1313 (1988).
[30] Empirically, the renormalized scattering rate $\tau^{-1}(m/m^*)$ rather than τ^{-1} appears to show the ω-linear dependence.
[31] T. Moriya, Y. Takahashi, and K. Ueda, J. Phys. Soc. Jpn. **49**, 2905 (1990).
[32] D. Pines, in *High Temperature Superconductivity*, edited by K. Bedell *et al.*, (Addison-Wesley, Redwood City, 1990), p. 240; D. Monthouxs and D. Pines, Phys. Rev. B **49**, 4261 (1994).
[33] A. Virosztek and J. Ruvalds, Phys. Rev. B **42**, 4064 (1990).
[34] C. M. Varma *et al.*, Phys. Rev. Lett. **63**, 1996 (1989).
[35] M. Gurvitch and A. T. Fiory, Phys. Rev. Lett. **59**, 1337 (1987).
[36] H. Eskes, M. B. J. Meinders, and G. A. Sawatzky, Phys. Rev. Lett. **67**, 1035 (1991); H. Eskes and A. M. Oles, *ibid.* **73**, 1279 (1994).
[37] W. Stephan and P. Horsch, Phys. Rev. B **42**, 8736 (1990).
[38] S. Maekawa, Y. Ohta, and T. Tohyama, in *Physics of High-Temperature Superconductors*, edited by S. Maekawa and M. Sato (Springer, Berlin, 1991), p. 29.
[39] For a review of the numerical calculations, see E. Dagotto, Rev. Mod. Phys. **66**, 763 (1994).
[40] S. Uchida, H. Eisaki, and S. Tajima, Physica B **186–188**, 975 (1993).
[41] H. Takagi *et al.*, Phys. Rev. Lett. **69**, 2975 (1992).
[42] T. Ito, K. Takenaka, and S. Uchida, Phys. Rev. Lett. **70**, 3995 (1993).
[43] H. Yasuoka, T. Imai, and T. Shimizu, in *Strong Correlation and Superconductivity*, edited by H. Fukuyama, S. Maekawa, and A. P. Malozemoff (Springer-Verlag, Berlin, 1989), p. 254.
[44] M. Takigawa *et al.*, Phys. Rev. B **43**, 247 (1991).
[45] J. Rossat-Mignod *et al.*, Physica C **185–189**, 86 (1991).
[46] P. M. Gehring *et al.*, Phys. Rev. B **44**, 2811 (1991).
[47] D. C. Johnston, Phys. Rev. Lett. **62**, 957 (1989).
[48] R. Yoshizaki *et al.*, Physica C **166**, 417 (1990).
[49] Y. Nakazawa and M. Ishikawa, Physica C **162–164**, 83 (1989).
[50] T. Nakano *et al.*, Phys. Rev. B **49**, 16 000 (1994).
[51] H. Y. Hwang *et al.*, Phys. Rev. Lett. **72**, 2636 (1994).
[52] H. L. Kao, J. Kwo, H. Takagi, and B. Batlogg, Phys. Rev. B **48**, 9925 (1993).
[53] K. Takenaka, K. Mizuhashi, H. Takagi, and S. Uchida, Phys. Rev. B **50**, 6534 (1994).
[54] L. Forro, Phys. Lett. A **179**, 140 (1993); C. Kendziora *et al.*, Phys. Rev. B **48**, 3531 (1993).
[55] S. Tajima *et al.*, J. Opt. Soc. Am. B **6**, 475 (1989).
[56] C. T. Chen *et al.*, Phys. Rev. Lett. **68**, 2543 (1992).
[57] E. Pellegrin *et al.*, Phys. Rev. B **47**, 3354 (1993).
[58] K. Tamasaku, T. Ito, H. Takagi, and S. Uchida, Phys. Rev. Lett. **72**, 3088 (1994).
[59] The evaluation of the critical interplane conductivity is based on a model given by M. Liu and D. Y. Xing, Phys. Rev. B **49**, 682 (1994).
[60] P. G. Radaelli *et al.*, Phys. Rev. B **49**, 4163 (1994).
[61] A. P. Litvinchuk, C. Thomsen, and M. Cardona, Solid State Commun. **80**, 257 (1991).
[62] A. P. Litvinchuk, C. Thomsen, and M. Cardona, Solid State Commun. **83**, 343 (1992).
[63] C. C. Homes *et al.*, Phys. Rev. Lett. **71**, 1645 (1993).
[64] D. N. Basov, T. Timusk, B. Dabrowski, and J. D. Jorgensen, Phys. Rev. B **50**, 3511 (1994).
[65] M. Reedyk, T. Timusk, J. S. Xue, and J. E. Greedan, Phys. Rev. B **49**, 15 984 (1994).
[66] J. Schützmann, S. Tajima, S. Miyamoto, Y. Sato, and R. Hauff, Phys. Rev. B **52**, 13 665 (1995).
[67] S. Uchida, Physica C **185–189**, 28 (1991).
[68] R. T. Collins *et al.*, Phys. Rev. B **39**, 6571 (1989).
[69] L. D. Rotter *et al.*, Phys. Rev. Lett. **67**, 2741 (1991).
[70] S-W. Cheong *et al.*, Phys. Rev. Lett. **67**, 1791 (1991).
[71] R. J. Birgeneau *et al.*, Phys. Rev. B **39**, 2868 (1989).
[72] P. B. Allen, W. E. Pickett, and H. Krakauer, Phys. Rev. B **37**, 7482 (1988).
[73] S. L. Cooper *et al.*, Phys. Rev. Lett. **70**, 1533 (1993); Phys. Rev. B **47**, 8233 (1993).
[74] M. Imada, J. Phys. Soc. Jpn. **63**, 3059 (1994).
[75] J. M. Wheatley, T. C. Hsu, and P. W. Anderson, Phys. Rev. B **37**, 5897 (1987); P. W. Anderson and Z. Zou, Phys. Rev. Lett. **60**, 132 (1988).
[76] N. Nagaosa, J. Phys. Chem. Solids **53**, 1493 (1992), and unpublished work.

[77] B. L. Altshuler and L. B. Ioffe, Solid State Commun. **82**, 253 (1992).
[78] M. Imada, Physica B **186–188**, 822 (1993).
[79] M. U. Ubbens and P. A. Lee, Phys. Rev. B **50**, 438 (1994).
[80] N. Kumar and A. M. Jayannavar, Phys. Rev. B **45**, 5001 (1992).
[81] M. J. Graf, D. Rainer, and J. A. Sauls, Phys. Rev. B **47**, 12 089 (1993).
[82] A. G. Rojo and K. Levin, Phys. Rev. B **48**, 16 861 (1993); R. J. Radtke, V. N. Kostur, and K. Levin, *ibid.* **53**, R522 (1996).
[83] P. Nyhus *et al.*, Phys. Rev. B **50**, 13 898 (1994).
[84] G. Kotliar *et al.*, Europhys. Lett. **15**, 655 (1991).
[85] Y. Fukuzumi, K. Mizuhashi, and S. Uchida (unpublished).
[86] N. Kumar, P. A. Lee, and B. Shapiro, Physica A **168**, 447 (1990).
[87] A. J. Leggett, Braz. J. Phys. **22**, 129 (1992).
[88] L. B. Ioffe, A. I. Larkin, A. A. Varlamov, and L. Yu, Phys. Rev. B **47**, 8936 (1993).
[89] T. Pham *et al.*, Phys. Rev. B **44**, 5377 (1991).
[90] D. Miller and P. L. Richards, Phys. Rev. B **47**, 12 308 (1993).
[91] Y. J. Uemura *et al.*, Phys. Rev. Lett. **62**, 2317 (1989).
[92] D. R. Harshman and A. P. Mills, Jr., Phys. Rev. B **45**, 10 684 (1992).
[93] Ch. Niedermayer *et al.*, Phys. Rev. Lett. **71**, 1764 (1993).
[94] Y. J. Uemura *et al.*, Nature **364**, 605 (1993).
[95] B. Koch *et al.*, Solid State Commun. **71**, 495 (1989).
[96] J. Münzel *et al.*, Physica C **235–240**, 1087 (1994).
[97] A. M. Gerrits *et al.*, Physica C **235–240**, 1117 (1994).
[98] D. van der Marel *et al.*, Physica C **235–240**, 1145 (1994).
[99] M. Tinkham, *Introduction to Superconductivity* (McGraw-Hill, New York, 1975).
[100] P. W. Anderson, in *Weak Superconductivity: The Josephson Tunneling Effect*, edited by E. R. Caianello (Academic Press, New York, 1964), Vol. 2, p. 113.
[101] L. N. Bulaevskii, M. P. Maley, and M. Tachiki, Phys. Rev. Lett. **74**, 801 (1995).
[102] M. Tachiki, T. Koyama, and S. Takahashi, Phys. Rev. B **50**, 7065 (1994).
[103] J. R. Clem, Physica C **162–164**, 1137 (1989).
[104] L. M. Bulaevski, Sov. Phys. JETP **37**, 1133 (1973); V. Ambegaokar and A. Baratoff, Phys. Rev. Lett. **10**, 486 (1963); **11**, 104 (1963).
[105] T. Shibauchi *et al.*, Phys. Rev. Lett. **72**, 2263 (1994).
[106] P. J. Hirschfeld *et al.*, Phys. Rev. B **40**, 6695 (1989).
[107] K. Kumagai *et al.*, Hyperfine Interact. **79**, 929 (1993).
[108] G. M. Luke *et al.*, Physica C **185–189**, 1175 (1991).
[109] K. Kumagai *et al.*, Physica C **185–189**, 913 (1991).
[110] T. E. Mason *et al.*, Phys. Rev. Lett. **71**, 919 (1993).
[111] J. Schützmann, S. Tajima, S. Miyamoto, and S. Tanaka, Phys. Rev. Lett. **73**, 174 (1994).
[112] S. Tajima, J. Schützmann, and S. Miyamoto, Solid State Commun. **95**, 759 (1995).
[113] C. Bernhard *et al.*, Physica C **226**, 250 (1994).
[114] P. W. Anderson, Science **268**, 1154 (1995).
[115] V. J. Emery and S. A. Kivelson, Nature **374**, 434 (1995).